JVI Accepts, published online ahead of print on 28 May 2014
J. Virol. doi:10.1128/JVI.01192-14

Particle Conformation Regulates Antibody Access to a Conserved GII.4 Norovirus Blockade Epitope.

Lisa C. Lindesmith[1], Eric F. Donaldson[1], Martina Beltramello[2], Stefania Pintus[2] Davide Corti[2,3], Jesica Swanstrom[1], Kari Debbink[1], Taylor A. Jones[1], Antonio Lanzavecchia[2,4], Ralph S. Baric[1]

[1]Department of Epidemiology, University of North Carolina, Chapel Hill, NC

[2]Institute for Research in Biomedicine, Bellinzona, Switzerland

[3] Humabs BioMed SA, Bellinzona, Switzerland

[4] Institute of Microbiology, ETH Zurich, 8093 Zurich, Switzerland

Short Title: Particle Conformation Impacts NoV Antibody Blockade

Corresponding author: Ralph S. Baric

3304 Hooker Research Center

135 Dauer DR

CB7435

School of Public Health

University of North Carolina-Chapel Hill

Chapel Hill, NC 27599

919-966-3895 (office)

919-966-0584 (fax)

rbaric@email.unc.edu

Abstract word count: 232

Text word count: 6927

Abstract

GII.4 noroviruses (NoVs) are the primary cause of epidemic viral acute gastroenteritis. One primary obstacle to successful NoV vaccination is the extensive degree of antigenic diversity among strains. The major capsid protein of GII.4 strains is evolving rapidly, resulting in the emergence of new strains with altered blockade epitopes. In addition to characterizing these evolving blockade epitopes, we have identified monoclonal antibodies (mabs) that recognize a blockade epitope conserved across time-ordered GII.4 strains. Uniquely, blockade potency of mabs that recognize the conserved GII.4 blockade epitope was temperature sensitive suggesting that particle conformation may regulate functional access to conserved, blockade, non-surface-exposed epitopes. To map conformation regulating motifs, we used bioinformatics tools to predict conserved motifs within the protruding domain of the capsid and designed mutant VLPs to test the impact of substitutions in these motifs on antibody cross-GII.4-blockade. Charge substitutions at residues 310, 316, 484 and 493 impacted blockade potential of cross-GII.4 blockade mabs, with minimal impact on blockade of mabs targeting other, separately evolving, blockade epitopes. Specifically, residue 310 modulated antibody blockade temperature sensitivity in tested strains. These data suggest access to the conserved GII.4 blockade antibody epitope is regulated by particle conformation, temperature, and amino acid residues positioned outside of the antibody binding site. The regulating motif is under limited selective pressure by the host immune response and may provide a robust target for broadly reactive NoV therapeutics and protective vaccines.

46 **Importance**

47 In this study, we explored the factors that govern norovirus cross-strain antibody
48 blockade. We found that access to the conserved GII.4 blockade epitope is regulated by
49 temperature and distal residues outside of the antibody binding site. These data are most
50 consistent with a model of NoV particle conformation plasticity that regulates antibody binding
51 to a distally conserved blockade epitope. Further, antibody "locking" of the particle into an
52 epitope accessible conformation prevents ligand binding, providing a potential target for broadly
53 effective drugs. These observations open lines of query into the mechanisms of human NoV
54 entry and uncoating, fundamental biological questions that are currently unanswerable for these
55 non-cultivatable pathogens.

56

Introduction

Noroviruses (NoVs) are the primary cause of severe acute viral gastroenteritis (1). In the United States alone, the annual NoV disease burden is estimated to be 2 billion dollars and 5,000 quality adjusted life years (2). Globally, NoV-associated deaths are estimated at 200,000 per year (3). Usually, disease severity is modest, but morbidity and mortality rates, particularly among the young, elderly, and immune-compromised are increasingly apparent (4-14). An effective vaccine would benefit not only these highly susceptible populations but also military, childcare, healthcare and food industry personnel. The primary obstacles to development of an effective NoV vaccine are the large number of antigenic variants, viral evolution, and an incomplete understanding of the components of protective immunity. A monovalent NoV vaccine based on Norwalk virus virus-like particles (VLPs) has demonstrated to be safe and effective at mitigating the risk of NoV illness and infection (15, 16). Although an important first step, additional studies that include NoV strains of more epidemiological relevance are needed to address the fundamental immunogenetic questions surrounding NoV susceptibility and protection from infection.

Strains from the GII.4 genotype cause 70-80% of norovirus outbreaks including four pandemics in the last 15 years. Strain US95/96 (GII.4.1997) mitigated the pandemic during the mid-1990's (17, 18), followed by the Farmington Hills strain (GII.4.2002) (19), the Hunter strain (GII.4.2004) (20-22), and the Minerva 2006b strain (GII.4.2006) (10, 21, 23). Although the number of documented outbreaks did not significantly increase, GII.4.2006b was subsequently replaced by the global circulating strain New Orleans (GII.4.2009) (1, 24). In 2012, the newly emerged Sydney strain (GII.4.2012) (25, 26) became the predominant circulating NoV strain, worldwide. This pattern of emergent strain replacement of a circulating strain followed by

periods of stasis is indicative of epochal evolution and results in new GII.4 strains with altered antigenicity and ligand binding profiles (27, 28). Importantly, of the NoVs studied, epochal evolution appears to be restricted to GII.4 NoV strains over the past 25 years.

Currently, there is no validated cell culture model for human norovirus cultivation. As members of the *Caliciviridae* family, NoVs contain positive-sense, single stranded RNA genomes of about 7.5 kb. Currently, there are five identified genogroups. Almost all human NoV infections are caused by strains from Genogroups (G) I and GII. Each of these genogroups is further subdivided into 9 and 21 different genotypes, respectively, based primarily on the amino acid sequence of the major capsid protein encoded by ORF 2 (29). When ORF2 is expressed *in vitro* an abundance of the major capsid protein is produced (30). Monomers of the major capsid protein first form dimers; then ninety dimers self-assemble into icosahedral virus-like particles (VLPs) that are morphologically and antigenically indistinguishable from native virions (31). The capsid protein itself is divided into three structural domains. The shell domain (S) forms the core of the particle and the protruding domain, which is divided into two subdomains; P1(residues 226-278 and 406-530) forms a stalk that extends away from the central core supporting the protruding subdomain 2 (P2, residues 279-405) (31). The P2 subdomain is the most surface-exposed region of the particle and has been shown to interact with potential neutralizing/blockade antibodies and carbohydrate binding ligands, such as synthetic histo-blood group antigens (HBGAs), human saliva, and pig gastric mucin (28, 32-36). In the GII.4 strains, residues of the P2 subdomain are under selective pressure by the host immune response; this pressure drives viral evolution resulting in antigenic drift and escape from herd immunity (28, 35, 37). The lack of a cell culture system for NoV propagation prompted us to develop an *in vitro* surrogate neutralization assay, or antibody "blockade" assay, that measures the capacity of

an antibody to block binding of a VLP to a carbohydrate ligand (28, 35, 38, 39). Importantly, the blockade assay has been verified by other groups as a surrogate neutralization assay in infected chimpanzees (40) and Norwalk virus-challenged people (15, 41). The surrogate neutralization "blockade" assay has been critical in mapping evolving GII.4 blockade antibody epitopes in strains antigenically too similar to be differentiated by enzyme immunoassay (EIA) (28, 42).

In addition to antigenic drift, several other viral factors correlate with new GII.4 strain emergence, including strain recombination (43) and polymerase fidelity (44, 45). Unfortunately, the absence of a standard infection model outside of humans, limits the possibility to study these mechanisms of viral immune evasion in depth. To date, only antigenic drift has been shown to directly impact the effectiveness of the human immune response to mitigate NoV infection. Using anti-GII.4 NoV human monoclonal antibodies (human mabs) we have mapped evolving GII.4 blockade epitopes (46, 47). Changes in these epitopes not only correlate with new strain emergence but also with loss of antibody blockade activity providing direct evidence that new GII.4 strains are serial human herd immunity escape variants. Many groups have used bioinformatics tools to predict potential GII.4 antibody epitopes (20, 27, 28, 48, 49). By coupling a large panel of anti-NoV monoclonal antibodies (mabs) with molecular genetic approaches we have validated three evolving GII.4 blockade epitopes. Epitope A (residues 294, 296-298, 368 and 372) is highly variable and changes with each new GII.4 strain emergence (35, 36, 46, 47). Epitope D (residues 393-395) is an evolving blockade epitope that also modulates HBGA binding of GII.4 strains providing mechanistic support for the observed correlation between epitope escape from herd immunity and altered HBGA binding (28, 47, 49). Epitope E (residues 407, 412 and 413) is a confirmed GII.4.2002 Farmington Hills-specific blockade epitope (36).

126 We have also described a GII.4-conserved, conformation-dependent blockade epitope
127 recognized by human mab NVB 71.4 (47). Although this epitope is conserved across GII.4
128 strains that circulated between 1987 and 2012, NVB 71.4 does not have equivalent blockade
129 capacity for all GII.4 VLPs, suggesting the antibody binds to a complex epitope comprised of
130 both conserved and variable residues. NVB 71.4 has diagnostic and therapeutic potential and
131 mapping of the epitope recognized by human mab NVB 71.4 may provide a target for widely
132 protective NoV drugs or vaccine design.
133 In this study, we demonstrate that antibody NVB 71.4 cross-blockade and access to the
134 conserved GII.4 blockade epitope is regulated by particle conformation, temperature and amino
135 acid residues positioned outside of the antibody binding site. Strategies to control particle
136 conformation changes will inform NoV immunogen presentation in VLP-based vaccines and
137 therapeutics.
138

Materials and Methods

Virus-like particles. Synthetically derived (Bio Basic INC, Amherst, NY) epitope-engineered or outbreak strain ORF2 genes were inserted directly into the VEE replicon vector for the production of virus replicon particles (VRPs), as described (35, 42). Bac-GII.4.2009 (New Orleans) VLPs were the kind gift of Dr. Jan Vinje, Centers for Disease Control and Prevention, Atlanta, GA and produced by expression in the baculovirus system and purified by cesium chloride gradient. Uranyl acetate stained VLPs were visualized by transmission electron microscopy (TEM). Scale bars (100 nm) are included in all micrographs for size reference. Of note, sequences used to produce VLPs were identified from stool samples from multiple infected individuals. Although irregular particles are occasionally seen in all VLP preparations regardless of the vector expression platform (28, 50), ORF2 proteins that self-assemble into plentiful ~40 nm spherical particles that retain robust binding to conformation-dependent monoclonal antibodies and carbohydrate ligands are considered validated for further studies.

Monoclonal Antibodies. The characteristics of the antibodies used in this study have been previously published except GII.4.2002.G5. Details are described in (47) for the human mabs and in (35, 51) for the mouse epitope A mabs. NVB 71.4 is a broad GII.4 blockade human mab isolated from a healthy blood donor. GII.4.2002.G5 is a mouse mab generated by hyperimmunization with GII.4.2002 VLPs, as described (36). This antibody is now commercially available from Maine Biotech (MAB227P). Fabs were obtained by papain cleavage using papain immobilized on beaded agarose resin (30 IU/mg) (Pierce) followed by

161 HiTrap protein-A (GE Healthcare) and size-exclusion chromatography (Superdex 200 from GE
162 Healthcare).
163
164 **Blocking Of Binding (BOB) Assay.** For experiments using human polyclonal serum, human
165 mabs were purified on protein A or G columns (GE Healthcare) and biotinylated using the EZ-
166 link NHS-PEO solid-phase biotinylation kit (Pierce). The competition between polyclonal serum
167 antibodies and biotinylated human mabs for binding to immobilized VLPs (1 µg/ml) was
168 measured by EIA. Briefly, plasma samples were added to GII.4.1997 or GII.4.2006-coated plates
169 at different dilutions. After 1 hour, biotinylated human mab was added at a concentration
170 corresponding to 80% of the maximal OD level, and the mixture was incubated at room
171 temperature for 1 hour. Plates were then washed with PBS-0.05% Tween-20 and bound
172 biotinylated humab was detected using AP-labeled streptavidin (Jackson Immunoresearch). The
173 percentage of inhibition was tested in duplicates and calculated as follows: (1−[(OD sample−OD
174 neg ctr) / (OD pos ctr−OD neg ctr)])×100. BD_{80} value was calculated by interpolation of curves
175 fitted with a 4-parameter nonlinear regression. For screening donor plasma samples and human
176 mab blocking of binding of mouse mabs, the binding titers to respective coated VLPs were
177 determined by EIA by measuring the dilution required to achieve 50% maximal binding (EC_{50})
178 as previously described (47). EIA plates were coated at 0.25 µg/ml VLP for human mab BOB of
179 mouse mab assays.
180
181 **Predicting Epitopes.** Guided by the empirical data observed for NVB 71.4 that indicated a
182 conserved GII.4 epitope was present, we reasoned that differential binding noted between GII
183 and GII.4 strains could be used to refine the search for a conserved region of the GII.4 capsid

sequence. Representatives of the capsid amino acid sequences of GII strains and GII.4 strains (28) from 1974 to 2012 were aligned using ClustalX version 2 (52) and the amino acid residues that were conserved among all GII capsid sequences and all GII.4 capsid sequences were mapped onto the GII.4.2004 (PDB accession: 3JSP) (53) crystal structure to identify areas that were conserved among all GII and all GII.4 capsid proteins. The original analysis was performed using the crystal structure for GII.4.1997 as the distances in the structure used for making the epitope prediction would be more reliable than in a homology model. The ERK and EHNQ motifs were identified as regions that were conserved among GII noroviruses, and highly conserved among GII.4 viruses. E316, R484, and K493 (ERK) and E488, H501, N522 and Q523 (EHNQ) were identified as conserved residues in these regions that carried a charge and had exposed side chains that protruded. These sites were targeted for mutagenesis using the rationale that preserving the charge of these residues would preserve the structural components necessary for VLP formation. Of note, epitope location predictions are based on VLP structures, not native virion structures.

VLP-Carbohydrate Ligand-Binding Assay.

EIA plates were coated with 10 µg/ml Pig Gastric Mucin (PGM) for 4 hours and blocked over night at 4ºC in 5% dry milk in PBS-0.05% Tween-20 before the addition of increasing concentrations of VLP. Bound VLP were detected by a rabbit anti-GII.4 norovirus polyclonal sera made from hyperimmunization with a cocktail of GII.4.1987, GII.4.2002, GII.4.2006 and GII.4.2009 VLPs, followed by anti-rabbit IgG-HRP (GE Healthcare) and color developed with 1-Step Ultra TMB ELISA HRP substrate solution (Thermo-Fisher). Each step was followed by washing with PBS-0.05% Tween 20 and all reagents were diluted in 5% dry milk in PBS-0.05%

Tween-20, pH 6.9. VLP binding to PGM is stable between pH 6.3 and 8.1, agreeing with previously published results (54). All incubations were done at room temperature. PGM at10 µg/ml is a saturating concentration and cannot distinguish carbohydrate affinities between VLPs but does give maximum binding potential of the entire panel of GII.4 VLPs. Half maximum binding (EC_{50}) values were calculated using sigmoidal dose response analysis of non-linear data in GraphPad Prism 6 (www.graphpad.com). Percent of maximum binding was compared to the mean OD 450 nm of 12 µg/ml VLP.

VLP-Carbohydrate Ligand-Binding Antibody Blockade Assay.

For blockade assays, PGM-coated plates were prepared as described above. VLPs (0.25 µg/ml) were pretreated with decreasing concentrations of test mab for 1 hour before being added to the carbohydrate ligand–coated plates for 1 hour. Wash steps and bound VLP were detected as described above. The percent control binding was defined as the binding level in the presence of antibody pretreatment compared to the binding level in the absence of antibody pretreatment multiplied by 100. Antibody-VLP and VLP-PGM incubations were done at room temperature or 37°C, as described for each figure. All other incubations were done at room temperature. Blockade data were fit using sigmoidal dose response analysis of non-linear data in GraphPad Prism 6. EC_{50} values were calculated for antibodies that demonstrated blockade of at least 50% at the dilution series tested. Monoclonal antibodies that did not block 50% of binding at the highest dilution tested were assigned an EC_{50} of 2X the assay upper limit of detection for statistical comparison. EC_{50} values between VLPs were compared using the One-way ANOVA with Dunnett posttest, when at least three values were compared or a student's T test when only two values were compared. A difference was considered significant if the P value was <0.05. Of

note, VLP concentrations in blockade assays are in the low nanomolar range and therefore cannot discriminate between antibodies with sub-nanomolar affinities. Antibody-VLP interactions were validated for compliance with the law of mass action by preforming blockade assays of GII.4.1997 and GII.4.2006 at 0.25, 0.5, 1 and 2 µg/ml VLP. EC_{50} values for antibody blockade varied less than 2-fold (1 dilution) between any combination of VLP concentration tested, indicating that under the test conditions, antibody is in excess to the VLP and the tenants of the law of mass action are met for the antibody-VLP binding (data not shown). Blockade assays using human type A or B saliva as the source of carbohydrate ligand were performed as described (55) with 0.5 µg/ml VLP at room temperature and 37°C.

Antibody relative affinity measurements. Antibody K_d measurements were done as previously described (56) at room temperature and 37°C. Serial dilutions were tested in duplicate in at least two independent experiments for each temperature. Briefly, EIA plates were coated with 0.25 µg/ml VLP in PBS, blocked, and incubated with serial dilutions of test antibody. Bound antibody was detected by anti-human IgG-HRP and color developed as described above. K_d values were calculated using one-site specific binding equation in GraphPad Prism 6. K_d values were validated by repeating the above assay at a range of VLP concentrations.

VLP-Protein A gold staining. VLPs were incubated with 5 µg/ml human mab at 37°C followed by 1/100 dilution of Protein A conjugated to 10 nm gold particles at room temperature, absorbed onto prepared grids, stained with 2% Uranyl acetate and visualized by TEM. Staining specificity was validated by counting fifty fields of the negative control (VLP minus human IgG plus Protein A-gold). Only one gold particle was observed near a VLP in the fifty negative control fields.

Results

Antibodies to conserved NoV epitopes are rarely detected in human serum samples. To estimate the fraction of antibodies specific for conserved GII.4 epitopes in the overall serum antibody response, one hundred serum samples collected from healthy individuals were assayed for ability to block binding of human mabs NVB 61.3 and NVB 71.4 in a blockade of binding (BOB) assay (57, 58). Both human mabs recognize a broad panel of antigenically-diverse, epidemiologically-significant GII.4 NoV strain VLPs by EIA but only NVB 71.4 blocks VLP-ligand interactions (47). When tested against GII.4.1997 **(Figure 1A)** or GII.4 2006 **(Figure 1B),** three sera were able to compete with NVB 61.3 binding by more than 80% while the remaining did not show significant inhibition, in spite of variable binding to tested VLPs (**Figure 1**, right column of each panel). Eighteen serum samples competed with NVB 71.4 binding to GII.4.1997 and six sera could compete for binding to GII.4.2006 by more than 80% (**Figure 1**). These data indicate that antibodies to GII.4 conserved epitopes may be rare in human serum samples even if the binding titers to the tested VLPs are high for the majority of the sera (EC_{50} value reported in the right column of each panel).

The conserved GII.4 blockade epitope is likely not surface exposed and antibody access to the epitope is regulated by particle conformation. To characterize the epitope recognized by NVB 71.4 we compared the profile for NVB 71.4 blockade of a time-ordered panel of GII.4 VLPs representing circulating GII.4 strains from 1987 through 2012. As shown previously (47), blockade curves had relatively shallow slopes (range 0.68-0.92) (**Figure 2A**). These data suggest that access of NVB 71.4 to the conserved blockade epitope may be restricted under the test conditions. Therefore, we repeated the blockade assay for NVB 71.4 against the panel of

GII.4 VLPs at 37°C to increase the probability of the VLPs adopting a conformation more favorable for antibody binding during the incubation time (59). Incubation at 37°C significantly increased the blockade capacity of NVB 71.4 for the panel of GII.4 VLPs (**Figure 2B**). Further, the blockade curves demonstrated steep slopes (range 1.1-2.8) with complete blockade reached at antibody saturation for each VLP. In agreement with previous findings (47), NVB 71.4 did not block each GII.4 VLP equivalently at room temperature or 37°C. Incubation at the higher temperature resulted in significantly less antibody needed for blockade of GII.4.1987 (21.4-fold less), GII.4.1997 (35.4-fold less), GII.4.2002 (5.0-fold less), GII.4.2006 (10.5-fold less), GII.4.2009 (6.9-fold less) and GII.4.2012 (9.9-fold less) (**Figure 2C**). Incubation at 37°C did not broaden the number of strains blocked by NVB 71.4, as the higher temperature did not allow blockade of any non-GII.4 VLPs tested (data not shown), in agreement with previous findings at room temperature (47). Temperature dependent NVB 71.4 blockade activity was confirmed with alternative ligand sources human type A and type B saliva (data not shown). As demonstrated for PGM, all of the tested VLPs were blocked at lower concentrations of NVB 71.4 at 37°C compared to RT. Although the temperature effect was retained across ligand sources, the degree of temperature effect varied by both GII.4 VLP and between the three types of ligand, in agreement with earlier reports (28, 47).

In contrast, EC_{50} titers for blockade of surface epitopes A and D were only minimally impacted by temperature. GII.4.2006 blockade by human mabs that bind to surface-exposed epitopes A and D required 1.4 and 1.3-fold less antibody, respectively, for 50% blockade of binding at 37°C compared to room temperature (data not shown). Although the mean EC_{50} titers for blockade of epitopes A and D are significantly different between room temperature and 37°C, the fold difference between the values reflects less than one two-fold serial dilution. These data

299 indicate that unlike epitopes A and D, the conserved blockade epitope recognized by NVB 71.4
300 may not be readily accessible on the viral particle at all times, resulting in regulated antibody
301 access under tested conditions.

302 In our screen of over 100 mouse mabs against GII.4 VLPs, we have identified only one
303 mab with broad GII.4 blockade activity and this cross-blockade was temperature dependent
304 (**Figure 3**). In agreement with NVB 71.4 findings, GII.4.2002.G5 mouse mab did not block each
305 GII.4 VLP equivalently at room temperature or 37^{o}C. Incubation at the higher temperature
306 resulted in less antibody needed for blockade of GII.4.1987 (46-fold less), GII.4.1997 (8.5-fold
307 less), GII.4.2002 (9.2-fold less), GII.4.2006 (10.2-fold less), GII.4.2009 (3.6-fold less) and
308 GII.4.2012 (3.9-fold less). Incubation at 37^{o}C did not broaden the number of strains blocked
309 (data not shown). The varied degrees of blockade between different GII.4 VLPs suggests that
310 the epitope GII.4.2002.G5 recognizes is composed of both residues that are conserved and
311 variable across the GII.4 panel, as observed for NVB 71.4 (**Figure 2**).

312 Viruses and virus-like particles are dynamic structures and the degree of structural
313 flexibility is temperature sensitive and can be influenced by host factors (59-61). While this
314 study is the first to show that VLPs produced from VEE replicons likely adopt different
315 conformations, to our knowledge no studies have demonstrated that viruses or VLPs assembled
316 in the baculovirus insect cell system which functions at 27-28°C, are similarly dynamic.
317 Therefore, we compared GII.4.2009 VLPs produced in the baculovirus-based insect system
318 (27°C) and the VEE-based mammalian system (37°C) for antibody blockade at room
319 temperature and 37°C. Importantly, the primary nucleotide sequence of both GII.4.2009 capsid
320 constructs is identical (GenBank accession number ADD10375). For both mammalian and
321 insect cell-produced GII.4.2009 VLPs, blockade of surface epitope A was efficient and not

temperature sensitive (≤ 1.3-fold less antibody needed for 50% blockade) (**Figure 4A**). Unexpectedly, NVB 71.4 blockade was also not temperature sensitive (1.3-fold more antibody at 37°C) for the insect cell-produced VLPs, compared to 6.9-fold less antibody needed at 37°C for the mammalian cell produced VLP. Further, NVB 71.4 blockade of GII.4.2009 VLP produced in insect cells required 29.3-fold less antibody for 50% blockade at room temperature and 3.2-fold less at 37°C compared to GII.4.2009 VLPs produced in mammalian cells (0.1133 and 0.1503 µg/ml compared to 3.322 at room temperature and 0.4817 µg/ml at 37°C (**Figures 4B** and **2** and (47)). GII.4.2002.G5 needed 93-fold less antibody at room temperature and 19-fold less at 37°C for 50% blockade for GII.4.2009 VLPs produced in insect cells compared to mammalian cells (0.0843 and 0.1173 µg/ml compared to 7.8 µg/ml at room temperature and 2.177 µg/ml at 37°C (**Figures 4C** and **3**). This lack of temperature effect on Bac-GII.4.2009 blockade was maintained when B saliva was used as the ligand source and when NVB 71.4 Fab fragments were used for the blocking antibody (data not shown). These data support other study findings suggesting that factors outside of the capsid sequence can modify VLP antigenicity in subtle ways and support the hypothesis that antibody access to the conserved GII.4 blockade epitope is regulated by temperature and likely particle conformation.

Prediction of a conserved GII.4 motif with epitope-like features. Using the crystal structure of GII.4.2004 P domain dimer (PDB accession: 3JSP) (53), conserved and variable amino acids were mapped onto the P domain dimer surface. A region that was highly conserved among GII.4 norovirus strains was identified on the side of the P domain dimer (**Figures 5A and B**), within the P1 subdomain, interior to the exposed surface of the P2 subdomain, and distal to the carbohydrate binding pockets that correlate with binding differences to NVB 71.4 (**Figures 5B and C**). This region contained several conserved amino acids in an area large enough to

represent a potential antibody binding site (>1000^2 Å), including charged amino acids at positions E316, R484, and K493 (post-1997 GII.4 numbering) (**Figure 5C**). These amino acids were named the ERK motif (**Figure 5C**). The ERK motif is highly conserved among GII.4 strains that circulated between 1987 and 2012 and was predicted to be either a binding site for or a regulator of NVB 71.4 binding. In addition, amino acid position 310 was identified as a site of variation among contemporary GII.4 epidemic strains (2009 and 2012) that was proximal to the highly conserved region containing the ERK motif (**Figure 5D**).

Conservation of the ERK motif and its sub-surface P1 location indicated that changes in these residues could be detrimental to viral particle structure or stability. Therefore, to evaluate the impact of the ERK motif on antibody blockade activity we designed mutant VLPs in the GII.4.2006 backbone that conserved the residue charge but changed the residue side chain length. The GII.4.2006.ERK clone contains substitutions E316D, R484K and K493R (**Figure 6A**). For comparison, we designed an additional P1 domain mutant based on a conserved GII antibody epitope recently published (62). GII.4.2006.EHNQ contains mutated residues E488D, H501K and N522Q and Q523N (post-1997 GII.4 numbering) (**Figure 6A**). The GII.4.2006.ERK substitutions did not notably alter particle structure as measured by electron microscopy visualization of ~40 nm spherical particles and ligand binding ability similar to GII.4.2006. However, microscopic visualization of GII.4.2006.EHNQ mutant revealed numerous irregular structures but no ~40nm spherical particles. Corresponding to the lack of particle integrity, this mutant was unable to bind carbohydrate ligand (**Figure 6B** and **C**). Having failed VLP manufacturing quality control, no additional studies were performed with mutant GII.4.2006.EHNQ.

The GII.4 conserved ERK motif impacts NVB 71.4 and GII.4.2002.G5 blockade capacity with little impact on temperature sensitivity. As the substitutions made within GII.4.2006.ERK retained ligand binding activity, we evaluated the impact of these residue changes on the blockade potency of NVB 71.4, GII.4.2002.G5, and antibodies to surface exposed epitopes. ERK substitutions resulted in minimal increases in blockade ability for both epitope A and D antibodies (1.3-fold less antibody needed for 50% blockade at 37^{o}C compared to room temperature for both human mabs, data not shown). However, the ERK motif substitutions resulted in complete loss of blockade potency of NVB 71.4 at room temperature. Blockade potency was restored at 37^{o}C (2.519 μg/ml), although significantly more antibody was needed for blockade compared to GII.4.2006 (4.1-fold more antibody) (**Figure 7A**). Similarly, GII.4.2002.G5 did not block GII.4.2006.ERK at room temperature but gained limited blockade potency at 37°C (11.43 μg/ml) (**Figure 7B**). However, significantly more antibody was needed for blockade of GII.4.2006.ERK compared to GII.4.2006 even at the elevated temperature (3.6-fold more). Further, blockade of GII.4.2006 and GII.4.2006.ERK with NVB 71.4 Fab fragments was more potent (lower EC_{50} value) but similarly temperature sensitive compared to NVB 71.4 IgG. Notably, the EC_{50} values were 2.1-fold different at room temperature (1.758 verses 0.8052) and 1.4-fold different at 37°C (0.1807 compared to 0.1259), indicating that with the smaller epitope-binding molecule, the ERK residues do not effect antigenicity (**Figure 7C**). Further, ERK substitutions negatively impact blockade potency for both conserved epitope antibodies but do not negate the compensatory effect of incubating at higher temperature, indicating that the ERK residues may be affecting antibody access to the epitope instead of the antibody binding strength for the epitope.

389 Quantitative EIAs (56) further indicate that ERK residue substitutions do not affect
390 antibody affinities. Based on the differences in blockade titer, if the ERK substitutions were
391 primarily affecting antibody affinity we would expect a 10-fold change in functional affinity for
392 NVB 71.4 at room temperature and a 4-fold change at 37°C. However, there is less than a two-
393 fold difference (one serial dilution) between antibody functional affinities (K_d values) of NVB
394 71.4, GII.4.2002.G5 and epitope D human mab for GII.4.2006 and GII.4.2006.ERK VLPs
395 between room temperature and 37°C (**Table 1**), clearly indicating that the ERK motif is not the
396 antibody biding site.

397 **Residue 310 modulates antibody blockade potency and temperature sensitivity.**
398 Dominant GII.4 strains circulating between 1987 and 2006 conserved an asparagine at residue
399 310. With the emergence of GII.4.2009, N310 became S310. Subsequently, GII.4.2012 replaced
400 the serine at 310 with an aspartic acid (**Figure 8B**). To investigate the role of residue 310 in
401 GII.4 VLPs, we first developed mutated VLPs that exchanged the 310 residue between
402 GII.4.2009 and 2012 (**Figure 9A**). These substitutions did not notably alter particle structure as
403 measured by electron microscopy visualization and ligand binding ability (**Figure 9B and C**) or
404 blockade by epitope A or D human mabs (data not shown). In these constructs the ERK motif
405 was unchanged. For both NVB 71.4 and GII.4.2002.G5, exchange of residue 310 between
406 GII.4.2009 and GII.4.2012 resulted in an exchange of potency and temperature sensitivity
407 phenotypes (**Figure 10A and B and dta not shown**). GII.4.2009.S310D blockade potency
408 decreased (2 and 4.1-fold) and temperature sensitivity increased 10.5 and 12-fold for NVB 71.4
409 and GII.4.2002.G5, respectively. Conversely, GII.4.2012.D310S blockade potency increased 2.7
410 and 3.2-fold and temperature sensitivity decreased 4.6 and 3.1-fold for each antibody. NVB 71.4
411 Fab had modestly increased potency at room temperature (1-2.8 fold) for the 310 mutant VLPs

and the blockade was less temperature sensitive (2.4-8.0 fold) compared to wildtype, indicating that the smaller molecule has better access to the epitope.

To evaluate the interplay between residue 310 and the ERK motif, we created VLP GII.4.2009.NERK containing both the S310D and ERK substitutions (S310D, E316D, R484K and K493R) (**Figure 9A**). This VLP is called NERK, instead of SERK because of the asparagine found at 310 in the GII.4 VLPs from 1987-2006. Interestingly, combining the 310 and ERK residue changes in the GII.4.2009 backbone resulted in a VLP that was similarly blocked as GII.4.2009 for NVB 71.4 but required 4.1-fold more GII.4.2002.G5 for 50% blockade. Of note, for both IgGs and NVB 71.4 Fab the NERK substitutions reduced the advantage of incubating at higher temperature by ~50% compared to wildtype VLP blockade. As there was less than a 2-fold difference in K_d values for NVB 71.4 or GII.4.2002.G5 binding to GII.4.2009 and GII.4.2009.NERK at room temperature or 37^{o}C (data not shown) it is unlikely that NERK forms the antibody epitope but instead that 310 and the ERK residues together form a regulating network. Blockade by anti-epitope A and D human mabs was unaffected by the 310 or NERK residue mutations indicating that the substitutions were specifically targeting the conserved blockade epitopes and not causing global particle disturbances (data not shown). These data indicate in multiple GII.4 backbones that residue 310 has a subtle effect on blockade potency at room temperature and a more significant effect on temperature sensitivity of the conserved blockade epitope. Comparison of the effect of serine verses aspartic acid at position 310 indicates better access to the epitope because of variation in regulating residues reduces the effect of incubating at higher temperature.

NVB 71.4 VLP-ligand interaction blockade is not explained by particle disassembly or steric hindrance. To explore the mechanisms of NVB 71.4 blockade we stained GII.4.2009 and

GII.4.2009.NERK VLPs with NVB 71.4 and epitope A human mabs and Protein A gold particles and observed antibody labeled VLPs by negative stain electron microscopy (**Figure 11**). Both NVB 71.4 and the epitope A human mabs labeled intact VLPs, indicating that the antibody-induced lack of ligand binding was not the result of antibody-mediated particle disassembly or that NVB 71.4 preferentially binds to disassembled capsid protein. To evaluate if NVB 71.4 binding to sub-surface sites altered the particle surface in a way that was undetectable by EM but rendered the particle unamenable to interactions at the surface, antibody blockade of binding competition assays were performed using antibodies to surface-exposed, conformation-dependent epitope A and sub-surface, conformation-dependent NVB 71.4 (**Figure 12**). When VLP coated plates were pre-incubated with an epitope A human mab, binding of a mouse epitope A mab was reduced. The epitope A human mab blocked 50% of binding of a mouse epitope A mab at 0.7325 µg/ml for GII.4.1997 and 0.1419 µg/ml for GII.4.2006. Binding of the epitope A human mab did not affect binding of the mouse mab GII.4.2002.G5 for either VLP. Likewise, a strain mismatched epitope A human mab did not affect binding of either the mouse epitope A or GII.4.2002.G5 antibody binding for either VLP. Conversely, pre-incubation of the VLP with NVB 71.4 did not affect binding of the mouse epitope A mabs but decreased binding of GII.4.2002.G5. NVB 71.4 human mab blocked 50% of binding of mouse GII.4.2002.G5 at 0.0982 µg/ml for GII.4.1997 and 0.1913 µg/ml for GII.4.2006. Combined, these data indicate that VLPs bound by NVB 71.4 retain conformation and spatial flexibility for interaction with molecules that bind to the particle surface, suggesting neither particle disassembly nor steric hindrance is likely to explain NVB 71.4 blockade activity.

Discussion

The extensive burden of NoV disease on both pre and post-industrialized nations warrants World Health Organization support for development of a NoV vaccine. A new GII.4 strain has emerged every 3-4 years since 2002 and the newly emergent strain, with altered blockade epitopes, has quickly spread globally thorough immunologically-naive populations, highlighting a significant hurdle to successful NoV vaccination regimens. Extensive work has documented the antigenic changes in epitope A that correlate with GII.4 strain emergence (35, 36, 42, 46) providing a possible surveillance target for NoV monitoring. Epitope D remained fairly static until GII.4.2012 Sydney mutations resulted in a loss of blockade activity by human mab NVB 97 (46). While the biological relevance of both epitopes A and D has been confirmed with human mabs, the natural variation within these epitopes makes them difficult targets for antigen-based vaccine design.

In comparison, blockade epitopes conserved among multiple epidemiologically important strains of virus, including herd-immunity escape mutants, provide potential targets for broadly protective vaccines and the antibodies that recognize these epitopes provide potential diagnostic and therapeutic reagents [50]. Recently, Hansman et al. (62) reported a linear GII NoV conserved antibody epitope that is exposed transiently by proposed changes in particle conformation. This antibody was not tested for blockade capacity and is unlikely to recognize the GII.4 conformation-dependent conserved blockade epitope. The conserved GII.4 blockade epitopes recognized by human mab NVB 71.4 and mouse mab GII.4.2002.G5 likely overlap but are not identical as NVB 71.4 can compete with GII.4.2002.G5 binding, but NVB 71.4 has a higher blockade capacity and a different preferential blockade pattern across a panel of time-ordered GII.4 VLPs.

480 The concept of viral capsids as dynamic structures that can assume different
481 conformations is a well-established assumption in virology. Herein, we map specific residues
482 that mediate possible conformation subsets, which may be important for manufacturing NoV
483 VLP based vaccines. Despite identifying residue changes that affect blockade capacity of NVB
484 71.4 and GII.4.2002.G5, we have not identified the epitope(s) that actually bind these mabs. For
485 both mabs, K_d and EC_{50} values were less than 2-fold different between GII.4.2006 and
486 GII.4.2006.ERK and while ERK substitutions decrease blockade potency of the antibodies they
487 do not eliminate the impact of elevated temperature on blockade. Further, blockade of
488 GII.4.2006 and GII.4.2006.ERK with NVB 71.4 Fab fragments reduces the effect of ERK
489 substitutions while maintaining the effect of temperature on blockade. These data clearly
490 indicate that the effect of the ERK motif on mab blockade is not the result of loss of antibody
491 binding to the epitope but instead suggest that ERK regulates antibody blockade capacity by
492 regulating functional access to the epitope itself. Previous work with polio virus (60) and West
493 Nile virus (59) has shown that temperature effects particle dynamics or "breathing" and
494 subsequently antibody access to non-surface epitopes. In both cases, at 37°C viruses are
495 dynamic structures reversibly exposing internal antibody epitopes that are concealed at 25°C.
496 Elegant studies with flaviviruses have carefully dissected the impact of residue changes, time,
497 and temperature on monoclonal antibody neutralization (59, 63). Similar to observations
498 reported here, for many antibodies the effect was less than one log of neutralization titer. Given
499 the limited impact of ERK changes on temperature dependence of blockade, the ERK domain
500 may lie near the antibody epitopes and influence blockade through an allosteric effect by altering
501 the environment surrounding the epitopes or it may conformation-shield the epitope from the
502 antibody. Why GII.4 NoVs occlude the conserved blockade epitope at room temperature but not

503 37°C is unknown but suggests that the epitope may be essential for infection and thus need to be
504 exposed in the host (37°C), but is also susceptible to degradation and thus needs to be protected
505 in the external environment where infection is not a viable option. In the absence of a feasible
506 infection model and GII.4 molecular clone, it is not possible to evaluate the relationship between
507 different particle conformations (epitope accessible verses not accessible) and infectious virus.
508 Blockade of residue 310 mutant VLPs indicate that 310 is a conformational regulator of access to
509 the conserved blockade epitopes in multiple GII.4 backgrounds. Comparing blockade of
510 GII.4.2009 (S310), GII.4.2006 (N310), GII.4.2012 (D310), GII.4.2009.S310D and
511 GII.4.2012.D310S VLPs, all in the context of the conserved ERK motif, supports a role for
512 residue 310 in accessibility of the conserved blockade epitope. Our data suggest that an aspartic
513 acid at position 310 limits access to the epitope more than a serine. Our structural analyses did
514 not have sufficient resolution to explain the impact of different amino acids at position 310.
515 Importantly, residue 310 exchanges did not completely recapitulate the wild type VLP blockade
516 temperature phenotype, suggesting that either additional residues likely impact antibody access
517 to the conserved GII.4 blockade epitope or residues within the actual epitope vary somewhat
518 between the two strains. Detailed crystallography studies of antibody-bound particles are needed
519 to answer these fundamental questions.

520 Although the mechanisms of antibody blockade of VLP-carbohydrate binding are not
521 known the correlation between antibody blockade titer and protection from infection and illness
522 has been documented (15, 41). The location of the ERK motif on the underside of the P domain,
523 suggests that NVB 71.4 and GII.4.2002.G5 do not block VLP-ligand interaction by providing a
524 physical barrier between the VLP and carbohydrate ligand, as is proposed for antibodies to the
525 surface-exposed epitopes A, D and E (**Figures 13**) (35, 36, 47). This hypothesis is supported by

observations that NVB 71.4 binding to VLP does not disrupt binding of antibody to surface epitope A and that antibody Fab fragments retain blockade activity for GII.4 VLPs. Blockade of VLP-ligand binding is also not a function of antibody-mediated particle disassembly or the result of the antibody binding to already disassembled particles, as mab staining of NVB 71.4-labeled VLPs only identified intact particles. Instead, we hypothesize that NVB 71.4 and GII.4.2002.G5 likely block VLP-ligand interaction by altering VLP conformation, i.e. by positioning the VLP in an epitope-accessible conformation (full antibody access to the conserved blockade epitope) that is unfavorable for ligand binding (**Figure 14**). Whether ligand binding is dependent upon the VLP being in an epitope-restricted conformation (limited antibody access to the conserved blockade epitope) or if the actual transition between epitope-accessible and epitope-restricted is key for ligand binding is yet to be determined. These results mimic well defined neutralization processes for antibodies that recognize conformation-shielded, conserved neutralization epitopes in a diverse group of RNA viruses, including the E protein DI domain of West Nile Virus (59, 64), the gp120 component of the Env protein of HIV (65, 66) and the Hemagglutinin stem of Influenza Virus type A (66, 67). Interestingly, each of these epitopes have residues in structural motifs that are either directly or indirectly involved in viral entry and fusion processes, further suggesting that the antibodies described here may neutralize GII.4 NoV strains by blocking the virus entry/uncoating mechanisms, although this is speculative.

Further study of GII.4.2009 VLP produced in an insect cell expression system at lower temperature provides support for the relationship between viral conformation and antibody blockade. Blockade of Bac-GII.4.2009 by NVB 71.4 and GII.4.2005.G5 is potent and not temperature dependent, suggesting that the native conformation of GII.4.2009 in this system highly favors the “epitope-accessible" form. Conversely, GII.4.2009 VLPs made in a

mammalian expression system at 37°C require more antibody for blockade and the blockade is temperature sensitive indicating that the particle assembly conditions can effect particle structure, epitope access and, subsequently, blockade potency for NVB 71.4 and GII.4.2002.G5. Even though the primary nucleotide sequence of the exogenous gene is identical in the insect cell vector and mammalian cell vector, multiple factors could explain the difference between the two GII.4.2009 VLPs including post-translational protein processing, although none of the NoV major capsid proteins studied to date have been found to be modified after production, temperature of particle assembly, and particle purification and storage conditions; all factors that could impact particle structure. Previous detailed studies of Norwalk virus VLPs produced in insect cells indicate that these VLPs undergo structural changes at high temperature (>50°C) and pH (>8) but are stable at the pH and temperatures of the blockade assay (68). How these studies with Norwalk virus VLPs relate to the GII.4 VLPs studied here is unknown as others have shown Norwalk and GII.4 VLPs have different pH-dependent ligand binding characteristics (54). In agreement with (54), pH did not affect ligand binding of GII.4 VLPs we tested (data not shown). Although temperature effects both kinetics and affinities of molecular interactions, temperature alone is unlikely to explain the difference, as VLPs made by infecting mammalian cells at 30°C with GII.4.2009 VRPs resulted in VLPs with the same antibody blockade potency and temperature dependence as VLPs made at 37°C from the same VRP. These data suggest that factors outside of the primary nucleotide sequence, including the host cell, may affect particle formation in subtle ways and antibody neutralization potential in significant ways. If the observed differences between the two GII.4.2009 VLPs studied here is the direct result of VLP production in the baculovirus vector system, this is key information for manufacturing of the baculovirus produced-VLP NoV vaccine currently in phase I study, as computational studies on

572 human papillomavirus suggest that limiting structural fluctuations should produce better vaccine
573 immunogens (69). While the Bac-GII.4.2009 VLPs clearly allow better antibody access to the
574 epitopes for NVB 71.4 and GII.4.2002.G5 compared to VLPs made using VRP in the
575 mammalian system, it seems likely that other sub-surface blockade epitopes will be less
576 accessible on the Bac-GII.4.2009 VLP. Detailed crystallography studies of antibody-bound
577 particles are needed to answer these fundamental questions about VLP structure and how it
578 impacts cross-strain blockade antibody responses. However, all of the crystallography studies on
579 NoV VLPs have been done on baculovirus or other non-mammalian cell culture derived proteins.
580 Given the observations presented here the field should consider evaluating VLPs produced in
581 additional mammalian based systems.

582 Antibodies to conserved GII.4 NoV blockade epitopes have important therapeutic and
583 vaccine potential. Human mab NVB 71.4 could be administered prophylactically for acute or
584 chronic illness (70). More importantly, the antibody could be used as a probe for antigen
585 panning to identify the conserved blockade epitope. The epitope could possibly then
586 subsequently be genetically engineered to have better access within an immunizing VLP. The
587 supposition that locking the VLP in an epitope-accessible conformation prevents ligand binding
588 suggests that a drug that could similarly lock viral conformation could be an effective broad
589 based NoV treatment, as has been described for rhinovirus treatment with WIN compounds (71).
590 Further, these observations open lines of query into the mechanisms of human NoV entry and
591 uncoating, presenting fundamental biological questions that are currently unanswerable for these
592 non-cultivatable pathogens.

593

Acknowledgements

The authors would like to thank Victoria Madden and C. Robert Bagnell JR of Microscopy Services Laboratory, Department of Pathology and Laboratory Medicine, University of North Carolina-Chapel Hill for expert technical support and David Jarrossay of the Institute for Research in Biomedicine, Bellinzona for cell sorting. This work was supported by a grant from the National Institutes of Health, Allergy and Infectious Diseases AI056351. The funders had no role in study design, data collection and analysis, decision to publish, or preparation of the manuscript.

References

1. 2011. Updated norovirus outbreak management and disease prevention guidelines. MMWR Recomm Rep **60:**1-18.
2. **Hoffmann S, Batz MB, Morris JG, Jr.** 2012. Annual cost of illness and quality-adjusted life year losses in the United States due to 14 foodborne pathogens. J Food Prot **75:**1292-1302.
3. **Patel MM, Widdowson MA, Glass RI, Akazawa K, Vinje J, Parashar UD.** 2008. Systematic literature review of role of noroviruses in sporadic gastroenteritis. Emerg Infect Dis **14:**1224-1231.
4. **Trivedi TK, Desai R, Hall AJ, Patel M, Parashar UD, Lopman BA.** 2013. Clinical characteristics of norovirus-associated deaths: a systematic literature review. Am J Infect Control **41:**654-657.
5. **Bok K, Green KY.** 2012. Norovirus gastroenteritis in immunocompromised patients. N Engl J Med **367:**2126-2132.
6. **Trivedi TK, DeSalvo T, Lee L, Palumbo A, Moll M, Curns A, Hall AJ, Patel M, Parashar UD, Lopman BA.** 2012. Hospitalizations and mortality associated with norovirus outbreaks in nursing homes, 2009-2010. Jama **308:**1668-1675.
7. **Hutson AM, Atmar RL, Estes MK.** 2004. Norovirus disease: changing epidemiology and host susceptibility factors. Trends Microbiol **12:**279-287.
8. **Estes MK, Prasad BV, Atmar RL.** 2006. Noroviruses everywhere: has something changed? Curr Opin Infect Dis **19:**467-474.

9. **Koopmans M, Vinj inverted question marke J, de Wit M, Leenen I, van der Poel W, van Duynhoven Y.** 2000. Molecular epidemiology of human enteric caliciviruses in The Netherlands. J Infect Dis **181 Suppl 2:**S262-269.

10. 2007. Norovirus activity--United States, 2006-2007. MMWR Morb Mortal Wkly Rep **56:**842-846.

11. **Okada M, Tanaka T, Oseto M, Takeda N, Shinozaki K.** 2006. Genetic analysis of noroviruses associated with fatalities in healthcare facilities. Arch Virol **151:**1635-1641.

12. **Harris JP, Edmunds WJ, Pebody R, Brown DW, Lopman BA.** 2008. Deaths from norovirus among the elderly, England and Wales. Emerg Infect Dis **14:**1546-1552.

13. **Schorn R, Hohne M, Meerbach A, Bossart W, Wuthrich RP, Schreier E, Muller NJ, Fehr T.** 2010. Chronic norovirus infection after kidney transplantation: molecular evidence for immune-driven viral evolution. Clin Infect Dis **51:**307-314.

14. **Hall AJ, Eisenbart VG, Etingue AL, Gould LH, Lopman BA, Parashar UD.** 2012. Epidemiology of foodborne norovirus outbreaks, United States, 2001-2008. Emerg Infect Dis **18:**1566-1573.

15. **Atmar RL, Bernstein DI, Harro CD, Al-Ibrahim MS, Chen WH, Ferreira J, Estes MK, Graham DY, Opekun AR, Richardson C, Mendelman PM.** 2011. Norovirus vaccine against experimental human Norwalk Virus illness. N Engl J Med **365:**2178-2187.

16. **Richardson C, Bargatze RF, Goodwin R, Mendelman PM.** 2013. Norovirus virus-like particle vaccines for the prevention of acute gastroenteritis. Expert Rev Vaccines **12:**155-167.

646 17. **Noel JS, Fankhauser RL, Ando T, Monroe SS, Glass RI.** 1999. Identification of a
647 distinct common strain of "Norwalk-like viruses" having a global distribution. J Infect
648 Dis **179:**1334-1344.
649 18. **Vinje J, Altena S, Koopmans M.** 1997. The incidence and genetic variability of small
650 round-structured viruses in outbreaks of gastroenteritis in the Netherlands. J Infect Dis
651 **176:**1374-1378.
652 19. **Widdowson MA, Cramer EH, Hadley L, Bresee JS, Beard RS, Bulens SN, Charles**
653 **M, Chege W, Isakbaeva E, Wright JG, Mintz E, Forney D, Massey J, Glass RI,**
654 **Monroe SS.** 2004. Outbreaks of acute gastroenteritis on cruise ships and on land:
655 identification of a predominant circulating strain of norovirus--United States, 2002. J
656 Infect Dis **190:**27-36.
657 20. **Bull RA, Tu ET, McIver CJ, Rawlinson WD, White PA.** 2006. Emergence of a new
658 norovirus genotype II.4 variant associated with global outbreaks of gastroenteritis. J Clin
659 Microbiol **44:**327-333.
660 21. **Kroneman A, Vennema H, Harris J, Reuter G, von Bonsdorff CH, Hedlund KO,**
661 **Vainio K, Jackson V, Pothier P, Koch J, Schreier E, Bottiger BE, Koopmans M.**
662 2006. Increase in norovirus activity reported in Europe. Euro Surveill **11:**E061214
663 061211.
664 22. **Phan TG, Kuroiwa T, Kaneshi K, Ueda Y, Nakaya S, Nishimura S, Yamamoto A,**
665 **Sugita K, Nishimura T, Yagyu F, Okitsu S, Muller WE, Maneekarn N, Ushijima H.**
666 2006. Changing distribution of norovirus genotypes and genetic analysis of recombinant
667 GIIb among infants and children with diarrhea in Japan. J Med Virol **78:**971-978.

668 23. **Siebenga J, Kroneman A, Vennema H, Duizer E, Koopmans M.** 2008. Food-borne
669 viruses in Europe network report: the norovirus GII.4 2006b (for US named Minerva-
670 like, for Japan Kobe034-like, for UK V6) variant now dominant in early seasonal
671 surveillance. Euro Surveill **13**.
672 24. **Vega E BL, Gregoricus N, Williams K, Lee D, Vinjé J.** 2011. Novel surveillance
673 network for norovirus gastroenteritis outbreaks, United States. Emerg Infect Dis.
674 **17:**1389-1395.
675 25. 2013. Emergence of new norovirus strain GII.4 Sydney--United States, 2012. MMWR
676 Morb Mortal Wkly Rep **62:**55.
677 26. **van Beek J, Ambert-Balay K, Botteldoorn N, Eden JS, Fonager J, Hewitt J, Iritani**
678 **N, Kroneman A, Vennema H, Vinje J, White PA, Koopmans M.** 2013. Indications for
679 worldwide increased norovirus activity associated with emergence of a new variant of
680 genotype II.4, late 2012. Euro Surveill **18:**8-9.
681 27. **Siebenga JJ, Vennema H, Renckens B, de Bruin E, van der Veer B, Siezen RJ,**
682 **Koopmans M.** 2007. Epochal Evolution of GGII.4 Norovirus Capsid Proteins from 1995
683 to 2006. J Virol **81:**9932-9941.
684 28. **Lindesmith LC, Donaldson EF, Lobue AD, Cannon JL, Zheng DP, Vinje J, Baric**
685 **RS.** 2008. Mechanisms of GII.4 norovirus persistence in human populations. PLoS Med
686 **5:**e31.
687 29. **Zheng DP, Ando T, Fankhauser RL, Beard RS, Glass RI, Monroe SS.** 2006.
688 Norovirus classification and proposed strain nomenclature. Virology **346:**312-323.
689 30. **Baric RS, Yount B, Lindesmith L, Harrington PR, Greene SR, Tseng FC, Davis N,**
690 **Johnston RE, Klapper DG, Moe CL.** 2002. Expression and self-assembly of norwalk

691 virus capsid protein from venezuelan equine encephalitis virus replicons. J Virol
692 **76:**3023-3030.
693 31. **Prasad BV, Hardy ME, Dokland T, Bella J, Rossmann MG, Estes MK.** 1999. X-ray
694 crystallographic structure of the Norwalk virus capsid. Science **286:**287-290.
695 32. **Chen R, Neill JD, Estes MK, Prasad BV.** 2006. X-ray structure of a native calicivirus:
696 structural insights into antigenic diversity and host specificity. Proc Natl Acad Sci U S A
697 **103:**8048-8053.
698 33. **Lochridge VP, Jutila KL, Graff JW, Hardy ME.** 2005. Epitopes in the P2 domain of
699 norovirus VP1 recognized by monoclonal antibodies that block cell interactions. J Gen
700 Virol **86:**2799-2806.
701 34. **Cao S, Lou Z, Tan M, Chen Y, Liu Y, Zhang Z, Zhang XC, Jiang X, Li X, Rao Z.**
702 2007. Structural Basis for the Recognition of Blood Group Trisaccharides by Norovirus. J
703 Virol **81:**549-557.
704 35. **Debbink K, Donaldson EF, Lindesmith LC, Baric RS.** 2012. Genetic mapping of a
705 highly variable norovirus GII.4 blockade epitope: potential role in escape from human
706 herd immunity. J Virol **86:**1214-1226.
707 36. **Lindesmith LC, Debbink K, Swanstrom J, Vinje J, Costantini V, Baric RS,**
708 **Donaldson EF.** 2012. Monoclonal antibody-based antigenic mapping of norovirus GII.4-
709 2002. J Virol **86:**873-883.
710 37. **Cannon JL, Lindesmith LC, Donaldson EF, Saxe L, Baric RS, Vinje J.** 2009. Herd
711 immunity to GII.4 noroviruses is supported by outbreak patient sera. J Virol **83:**5363-
712 5374.

38. **Harrington PR, Lindesmith L, Yount B, Moe CL, Baric RS.** 2002. Binding of Norwalk virus-like particles to ABH histo-blood group antigens is blocked by antisera from infected human volunteers or experimentally vaccinated mice. J Virol **76:**12335-12343.

39. **Lindesmith LC, Donaldson E, Leon J, Moe CL, Frelinger JA, Johnston RE, Weber DJ, Baric RS.** 2010. Heterotypic humoral and cellular immune responses following Norwalk virus infection. J Virol **84:**1800-1815.

40. **Bok K, Parra GI, Mitra T, Abente E, Shaver CK, Boon D, Engle R, Yu C, Kapikian AZ, Sosnovtsev SV, Purcell RH, Green KY.** 2011. Chimpanzees as an animal model for human norovirus infection and vaccine development. Proc Natl Acad Sci U S A **108:**325-330.

41. **Reeck A, Kavanagh O, Estes MK, Opekun AR, Gilger MA, Graham DY, Atmar RL.** 2010. Serological Correlate of Protection against Norovirus-Induced Gastroenteritis. The J Infect Dis **202:**1212-1218.

42. **Lindesmith LC, Costantini V, Swanstrom J, Debbink K, Donaldson EF, Vinje J, Baric RS.** 2013. Emergence of a Norovirus GII.4 Strain Correlates with Changes in Evolving Blockade Epitopes. J Virol **87:**2803-2813.

43. **Eden JS, Tanaka MM, Boni MF, Rawlinson WD, White PA.** 2013. Recombination within the pandemic norovirus GII.4 lineage. J Virol **87:**6270-6282.

44. **Bull RA, Eden JS, Rawlinson WD, White PA.** 2010. Rapid evolution of pandemic noroviruses of the GII.4 lineage. PLoS Pathog **6:**e1000831.

45. **Siebenga JJ, Lemey P, Kosakovsky Pond SL, Rambaut A, Vennema H, Koopmans M.** 2010. Phylodynamic reconstruction reveals norovirus GII.4 epidemic expansions and their molecular determinants. PLoS Pathog **6:**e1000884.

46. **Debbink K, Lindesmith LC, Donaldson EF, Costantini V, Beltramello M, Corti D, Swanstrom J, Lanzavecchia A, Vinje J, Baric RS.** 2013. Emergence of New Pandemic GII.4 Sydney Norovirus Strain Correlates With Escape From Herd Immunity. J Infect Dis. .**208:**1877-1887.

47. **Lindesmith LC, Beltramello M, Donaldson EF, Corti D, Swanstrom J, Debbink K, Lanzavecchia A, Baric RS.** 2012. Immunogenetic mechanisms driving norovirus GII.4 antigenic variation. PLoS Pathog **8:**e1002705.

48. **Allen DJ, Gray JJ, Gallimore CI, Xerry J, Iturriza-Gomara M.** 2008. Analysis of amino acid variation in the P2 domain of the GII-4 norovirus VP1 protein reveals putative variant-specific epitopes. PLoS ONE **3:**e1485.

49. **Donaldson EF, Lindesmith LC, Lobue AD, Baric RS.** 2008. Norovirus pathogenesis: mechanisms of persistence and immune evasion in human populations. Immunol Rev **225:**190-211.

50. **Belliot G, Noel JS, Li JF, Seto Y, Humphrey CD, Ando T, Glass RI, Monroe SS.** 2001. Characterization of capsid genes, expressed in the baculovirus system, of three new genetically distinct strains of "Norwalk-like viruses". J Clin Microbiol **39:**4288-4295.

51. **Lindesmith LC, Donaldson EF, Baric RS.** 2011. Norovirus GII.4 strain antigenic variation. J Virol **85:**231-242.

52. **Larkin MA, Blackshields G, Brown NP, Chenna R, McGettigan PA, McWilliam H, Valentin F, Wallace IM, Wilm A, Lopez R, Thompson JD, Gibson TJ, Higgins DG.** 2007. Clustal W and Clustal X version 2.0. Bioinformatics **23:**2947-2948.

53. **Shanker S, Choi JM, Sankaran B, Atmar RL, Estes MK, Prasad BV.** 2011. Structural Analysis of HBGA Binding Specificity in a Norovirus GII.4 Epidemic Variant: Implications for Epochal Evolution. J Virol **85:**8635-8645.

54. **Tian P, Yang D, Jiang X, Zhong W, Cannon JL, Burkhardt W, 3rd, Woods JW, Hartman G, Lindesmith L, Baric RS, Mandrell R.** 2010. Specificity and kinetics of norovirus binding to magnetic bead-conjugated histo-blood group antigens. J Appl Microbiol **109:**1753-1762.

55. **Swanstrom J, Lindesmith LC, Donaldson EF, Yount B, Baric RS.** 2014. Characterization of Blockade Antibody Responses in GII.2.1976 Snow Mountain Virus-Infected Subjects. J Virol **88:**829-837.

56. **Lee PD, Mukherjee S, Edeling MA, Dowd KA, Austin SK, Manhart CJ, Diamond MS, Fremont DH, Pierson TC.** 2013. The Fc region of an antibody impacts the neutralization of West Nile viruses in different maturation states. J Virol **87:**13729-13740.

57. **Corti D, Langedijk JP, Hinz A, Seaman MS, Vanzetta F, Fernandez-Rodriguez BM, Silacci C, Pinna D, Jarrossay D, Balla-Jhagjhoorsingh S, Willems B, Zekveld MJ, Dreja H, O'Sullivan E, Pade C, Orkin C, Jeffs SA, Montefiori DC, Davis D, Weissenhorn W, McKnight A, Heeney JL, Sallusto F, Sattentau QJ, Weiss RA, Lanzavecchia A.** 2010. Analysis of memory B cell responses and isolation of novel

777 monoclonal antibodies with neutralizing breadth from HIV-1-infected individuals. PLoS
778 ONE **5:**e8805.
779 58. **Sabin C, Corti D, Buzon V, Seaman MS, Lutje Hulsik D, Hinz A, Vanzetta F, Agatic**
780 **G, Silacci C, Mainetti L, Scarlatti G, Sallusto F, Weiss R, Lanzavecchia A,**
781 **Weissenhorn W.** 2010. Crystal structure and size-dependent neutralization properties of
782 HK20, a human monoclonal antibody binding to the highly conserved heptad repeat 1 of
783 gp41. PLoS Pathog **6:**e1001195.
784 59. **Dowd KA, Jost CA, Durbin AP, Whitehead SS, Pierson TC.** 2011. A dynamic
785 landscape for antibody binding modulates antibody-mediated neutralization of West Nile
786 virus. PLoS Pathog **7:**e1002111.
787 60. **Li Q, Yafal AG, Lee YM, Hogle J, Chow M.** 1994. Poliovirus neutralization by
788 antibodies to internal epitopes of VP4 and VP1 results from reversible exposure of these
789 sequences at physiological temperature. J Virol **68:**3965-3970.
790 61. **Nelson S, Jost CA, Xu Q, Ess J, Martin JE, Oliphant T, Whitehead SS, Durbin AP,**
791 **Graham BS, Diamond MS, Pierson TC.** 2008. Maturation of West Nile virus
792 modulates sensitivity to antibody-mediated neutralization. PLoS Pathog **4:**e1000060.
793 62. **Hansman GS, Taylor DW, McLellan JS, Smith TJ, Georgiev I, Tame JR, Park SY,**
794 **Yamazaki M, Gondaira F, Miki M, Katayama K, Murata K, Kwong PD.** 2012.
795 Structural basis for broad detection of genogroup II noroviruses by a monoclonal
796 antibody that binds to a site occluded in the viral particle. J Virol **86:**3635-3646.
797 63. **Vanblargan LA, Mukherjee S, Dowd KA, Durbin AP, Whitehead SS, Pierson TC.**
798 2013. The type-specific neutralizing antibody response elicited by a dengue vaccine

candidate is focused on two amino acids of the envelope protein. PLoS Pathog **9:**e1003761.

64. **Dowd KA, Pierson TC.** 2011. Antibody-mediated neutralization of flaviviruses: a reductionist view. Virology **411:**306-315.

65. **van Gils MJ, Sanders RW.** 2013. Broadly neutralizing antibodies against HIV-1: templates for a vaccine. Virology **435:**46-56.

66. **Corti D, Lanzavecchia A.** 2013. Broadly neutralizing antiviral antibodies. Annu Rev Immunol **31:**705-742.

67. **Stanekova Z, Adkins I, Kosova M, Janulikova J, Sebo P, Vareckova E.** 2013. Heterosubtypic protection against influenza A induced by adenylate cyclase toxoids delivering conserved HA2 subunit of hemagglutinin. Antiviral Res **97:**24-35.

68. **Ausar SF, Foubert TR, Hudson MH, Vedvick TS, Middaugh CR.** 2006. Conformational stability and disassembly of Norwalk virus-like particles. Effect of pH and temperature. J Biol Chem **281:**19478-19488.

69. **Singharoy A, Polavarapu A, Joshi H, Baik MH, Ortoleva P.** 2013. Epitope fluctuations in the human papillomavirus are under dynamic allosteric control: a computational evaluation of a new vaccine design strategy. J Am Chem Soc **135:**18458-18468.

70. **Chagla Z, Quirt J, Woodward K, Neary J, Rutherford C.** 2013. Chronic norovirus infection in a transplant patient successfully treated with enterally administered immune globulin. J Clin Virol **58:**306-308.

71. **Reisdorph N, Thomas JJ, Katpally U, Chase E, Harris K, Siuzdak G, Smith TJ.** 2003. Human rhinovirus capsid dynamics is controlled by canyon flexibility. Virology **314:**34-44.

825 **Figure Legends**

826 **Figure 1. Antibodies to conserved NoV epitopes are rare in human plasma**. The ability of
827 human serum samples (n=100) to block binding of human mabs was evaluated using a Blockade
828 of Binding (BOB) assay. Shown is the reciprocal plasma dilution that blocks 80% binding (BD_{80})
829 of a conserved GII non-blockade epitope antibody (NVB 61.3) and a conserved GII.4 blockade
830 epitope antibody (NVB 71.4) to GII.4.1997 (**Panel A**) and GII.4.2006 (**Panel B**) VLPs. Each
831 symbol represents a different individual. BD_{80} values <40 were scored as negative. Total serum
832 IgG binding to GII.4.1997 and GII.4.2006 was determined by EIA. Reciprocal EC_{50} values are
833 shown (right column Panel A and B). ▲Sera competing for binding of NVB 61.3; • Sera
834 competing for binding of NVB 71.4; ∗ Donor source of NVB 61.3 and 71.4.
835
836 **Figure 2. Access of NVB 71.4 to the conserved GII.4 blockade epitope is temperature**
837 **dependent.** NVB 71.4 was assayed for ability to block the interaction of a panel of time-ordered
838 GII.4 VLPs with carbohydrate ligand. Sigmoidal curves were fit to the mean percent control
839 binding (percent of VLP bound to ligand in the presence of antibody pretreatment compared to
840 the amount of VLP bound in the absence of antibody pretreatment) at room temperature (**Panel**
841 **A**) and 37°C (**Panel B**) and the mean EC_{50} (µg/ml) titers for blockade at room temperature (●)
842 and 37°C (●) calculated and compared (**Panel C**). The fold change in EC_{50} titer was defined as
843 the mean EC_{50} at 37°C compared to room temperature. * Mean EC_{50} blockade titer is
844 significantly different between room temperature and 37°C. Dashed line in Panel C marks the
845 assay upper limit of detection. Error bars represent the SEM on sigmoidal fit curves and 95%
846 confidence intervals on Mean EC_{50} graphs.

847

848 **Figure 3. Access of GII.4.2002.G5 to a conserved GII.4 blockade epitope is regulated by**
849 **temperature.** GII.4.2002.G5 was assayed for ability to block the interaction of GII.4 VLPs with
850 carbohydrate ligand at room temperature (●) and 37°C (●). Sigmoidal curves were fit to the
851 mean percent control binding (percent of VLP bound to ligand in the presence of antibody
852 pretreatment compared to the amount of VLP bound in the absence of antibody pretreatment) and
853 the mean EC_{50} (μg/ml) titer for blockade calculated. The fold change in EC_{50} titer was defined as
854 the mean EC_{50} at 37°C compared to room temperature. * Mean EC_{50} blockade titer is
855 significantly different between room temperature and 37°C. Non-blockade VLPs were assigned
856 an EC_{50} of 2X the upper limit of detection for statistical analysis and denoted by a data marker
857 on the graph above the dashed line (assay upper limit of detection) for visual comparison. Error
858 bars represent 95% confidence intervals.

859

860 **Figure 4. Antibody access to the conserved epitope is not temperature sensitive on**
861 **GII.4.2009 VLPs made at lower temperature in insect cells.** Epitope A human mab (**Panel**
862 **A**), NVB 71.4 (**Panel B**) and GII.4.2002.G5 (**Panel C**) were assayed for ability to block the
863 interaction of GII.4.2009 VLPs produced in insect cells using a baculovirus expression system
864 and carbohydrate ligand at room temperature (●) and 37°C (●). Sigmoidal curves were fit to the
865 mean percent control binding (percent of VLP bound to ligand in the presence of antibody
866 pretreatment compared to the amount of VLP bound in the absence of antibody pretreatment) and
867 the mean EC_{50} (μg/ml) titer for blockade calculated. The fold change in EC_{50} titer was defined as
868 the mean EC_{50} at 37°C compared to room temperature. * Mean EC_{50} blockade titer is

869 significantly different between room temperature and 37°C. Error bars represent 95% confidence
870 intervals.
871
872 **Figure 5. Predicting a conserved epitope.** This figure shows Chain A (dark blue) and Chain B
873 (light blue) of the protruding domain structure. The P1 subdomain is highly conserved among
874 GII.4 epidemic strains and is hidden from the surface in the context of the VLP superstructure.
875 The carbohydrate binding pocket (pink) is located in the P2 subdomain, which is exposed on the
876 surface of the VLP (**Panel A**). A conserved region was identified on the side of the P domain
877 dimer, distal to the binding pockets with sites of variation (red) that correlated with phenotypic
878 differences among GII.4 VLPs (**Panel B**). The ERK motif (**Panel C**, rotated 60°
879 counterclockwise on the X-axis compared to Panel B) is comprised of three charged amino acids
880 that are found at positions 316, 484, and 493 (red) in the conserved region (encompassed in the
881 red line) that is predicted to interact with NVB 71.4. Variation at position 310 (yellow) is
882 proximal to the conserved region (**Panel D**) and may regulate binding to this conserved site.
883
884 **Figure 6. Characterization of VLPs with substitutions in predicted conserved antibody**
885 **epitopes.** Schematic of constructs (**Panel A**). Particle integrity was verified by transmission
886 electron microscope visualization (**Panel B**) and carbohydrate ligand (Pig Gastric Mucin type III,
887 PGM) binding of VLPs (**Panel C**). Non-PGM binding VLPs were assigned an EC_{50} of 2X the
888 upper limit of detection for statistical analysis and denoted by a data marker on the graph above
889 the dashed line (assay upper limit of detection) for visual comparison. Error bars represent 95%
890 confidence intervals.
891

892 **Figure 7. ERK motif substitutions decrease NVB 71.4 and GII.4.2002.G5 blockade**
893 **potential with little impact on blockade temperature sensitivity.** NVB 71.4 (**Panels A and D**),
894 GII.4.2002.G5 (**Panels B and E**) and NVB 71.4 Fab (**Panels C and F**) were assayed for ability
895 to block carbohydrate ligand interaction of GII.4.2006 VLPs at room temperature (●) and 37 °C
896 (■) and GII.4.2006.ERK VLPs at room temperature (●) and 37 °C (■). Sigmoidal curves were fit
897 to the mean percent control binding (percent of VLP bound to ligand in the presence of antibody
898 pretreatment compared to the amount of VLP bound in the absence of antibody pretreatment) and
899 the mean EC_{50} (μg/ml) titer for blockade calculated and compared. The fold change in EC_{50} titer
900 was defined as the mean EC_{50} at 37 °C compared to room temperature. * Mean EC_{50} blockade
901 titer for GII.4.2006.ERK significantly different from the mean EC_{50} blockade titer for GII.4.2006
902 at the same temperature. Non-blockade VLPs were assigned an EC_{50} of 2X the upper limit of
903 detection for statistical analysis and denoted by a data marker on the graph above the dashed line
904 (assay upper limit of detection) for visual comparison. Error bars represent the SEM on
905 sigmoidal fit curves and 95% confidence intervals on Mean EC_{50} graphs.
906
907 **Figure 8. Predicting residues that interact with the ERK motif.** The ERK motif was mapped
908 onto the crystal structure of GII.4.2004 to identify sites that may be interacting with the ERK
909 motif (**Panel A**). The ERK motif is highly conserved among epidemiologically important GII.4
910 strains while residue 310 has evolved in the most recent GII.4 strains with global distribution
911 (**Panel B**).
912

913 **Figure 9. Characterization of VLPs with substitutions in residue 310 and NERK.**
914 Schematic of constructs (**Panel A**). Particle integrity was verified by transmission electron
915 microscope visualization (**Panel B**) and carbohydrate ligand (PGM) binding of VLPs (**Panel C**).
916 Dashed line marks the upper limit of detection in Panel C. Error bars represent 95% confidence
917 intervals.
918
919 **Figure 10. Residue 310 inversely modulates blockade potency and temperature sensitivity**
920 **of the conserved GII.4 epitope.** GII.4.2002.G5 (**Panels A and B**), and NVB 71.4 Fab
921 fragments, and NVB 71.4 IgG (**Panel B**) were assayed for ability to block the interaction of
922 VLPs with carbohydrate ligand at room temperature and (●) and 37 °C (●). Sigmoidal curves
923 were fit to the mean percent control binding (percent of VLP bound to ligand in the presence of
924 antibody pretreatment compared to the amount of VLP bound in the absence of antibody
925 pretreatment) and the mean EC_{50} (μg/ml) titer for blockade calculated. The fold change in
926 potency (EC_{50} titer) was defined as the ratio between mutant VLPs and wildtype VLP at room
927 temperature (**Panels A and B**). The fold change in temperature sensitivity was defined as the
928 change in ratio between mean EC_{50} at 37 °C compared to room temperature for the mutant VLP
929 compared to ratio at both temperatures for the wildtype VLP (**Panel B**). * Mean EC_{50} blockade
930 titer for mutant VLP significantly different from the mean EC_{50} blockade titer for wildtype VLP
931 at the same temperature. Error bars represent 95% confidence intervals. ■ Fold increase. ■ Fold
932 decrease.
933
934 **Figure 11. Antibody-bound VLPs retain structural integrity.** GII.4.2009 (**Panel A**) and
935 GII.4.2009.NERK (**Panel B**) VLPs were immuno-stained with NVB 71.4 or epitope A

936 (GII.4.2009 only, **Panel C**) humabs and visualized by negative stain transmission electron
937 microscopy. Arrows denote immuno-gold labeled VLPs.
938
939 **Figure 12. Binding of NVB 71.4 does not disrupt surface epitope A topology.** Human mabs
940 to surface epitope A or NVB 71.4 were evaluated for ability to block binding of mouse mabs to
941 epitope A or the conserved blockade epitope in GII.4.1997 (**Panel A**) and GII.4.2006 (**Panel B**)
942 using a BOB assay. Sigmoidal curves were fit to the mean percent control binding (percent of
943 mouse mab bound to VLP in the presence of human mab pretreatment compared to the amount
944 of mouse mab bound in the absence of human mab pretreatment) and the mean EC_{50} (µg/ml) titer
945 for blockade of binding calculated. ■ EC_{50} > 8µg/ml, ■ EC_{50} < 1µg/ml.
946
947 **Figure 13. The mapped epitopes of GII.4 noroviruses.** The previously described evolving
948 antibody blockade epitopes A-E are shown on the surface next to the carbohydrate binding sites
949 (pink) (**Panel A**). The NERK motif is shown in red (red) and is distal to the carbohydrate
950 binding sites (pink) (**Panel B**).
951
952 **Figure 14. Proposed model for regulation of antibody access to the conserved GII.4**
953 **blockade epitope/s by the NERK motif and VLP structural conformation.** GII.4 NoV VLPs
954 produced in mammalian cells can exist in multiple conformations. Two possibilities are
955 represented here by the light and dark green VLP shading. Antibody access to the conserved
956 GII.4 blockade epitope is different between these states. Antibody "locking" of the particle into
957 an epitope accessible conformation prevents ligand binding and antibody blockade activity.
958 Further, antibody access to the conserved GII.4 blockade epitope can be regulated by

959 temperature and residues outside of the antibody binding site. Elevated temperature or a serine
960 at residue 310 favors antibody access to the epitope and subsequently more blockade activity
961 whereas lower temperature or an aspartic acid at position 310 restricts antibody access to the
962 epitope resulting less blockade activity.
963

964 **Tables**

965 **TABLE 1** Monoclonal antibody functional affinities for GII.4.2006 and GII.4.2006.ERK at

966 room temperature and 37°C

mab	Temp (°C)	GII.4.2006 K_d (nM ± SEM)	GII.4.2006.ERK K_d (nM ±SEM)
NVB 71.4	RT	0.48 ± 0.09	0.56 ± 0.01
NVB 71.4	37	0.27 ± 0.01	0.29 ± 0.05
GII.4.2002.G5	RT	1.0 ± 0.24	2.0 ± 0.29
GII.4.2002.G5	37	0.57 ± 0.05	0.87 ± 0.11
Epitope D	RT	0.78 ± 0.09	0.95 ± 0.13
Epitope D	37	0.39 ± 0.07	0.41 ± 0.05

967

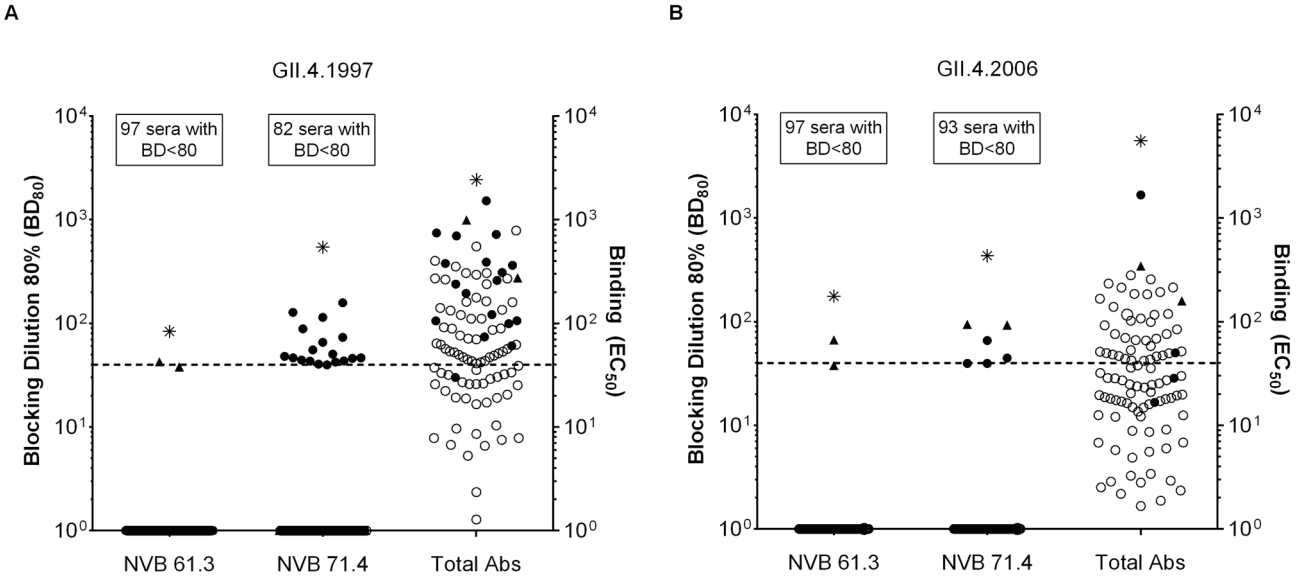

A

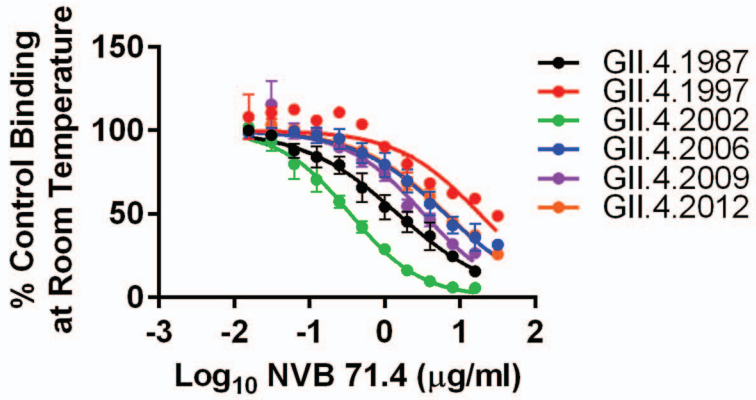

B

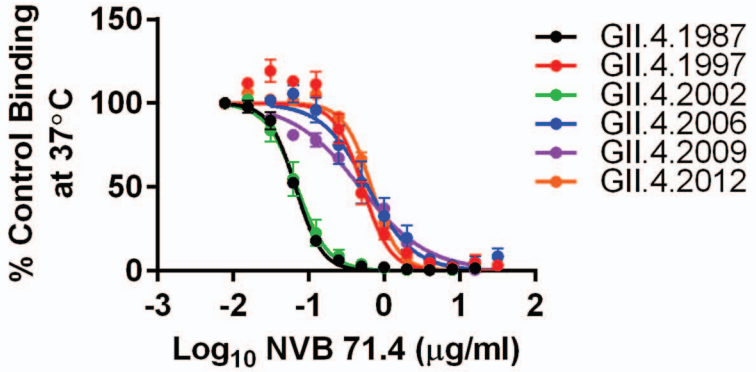

C

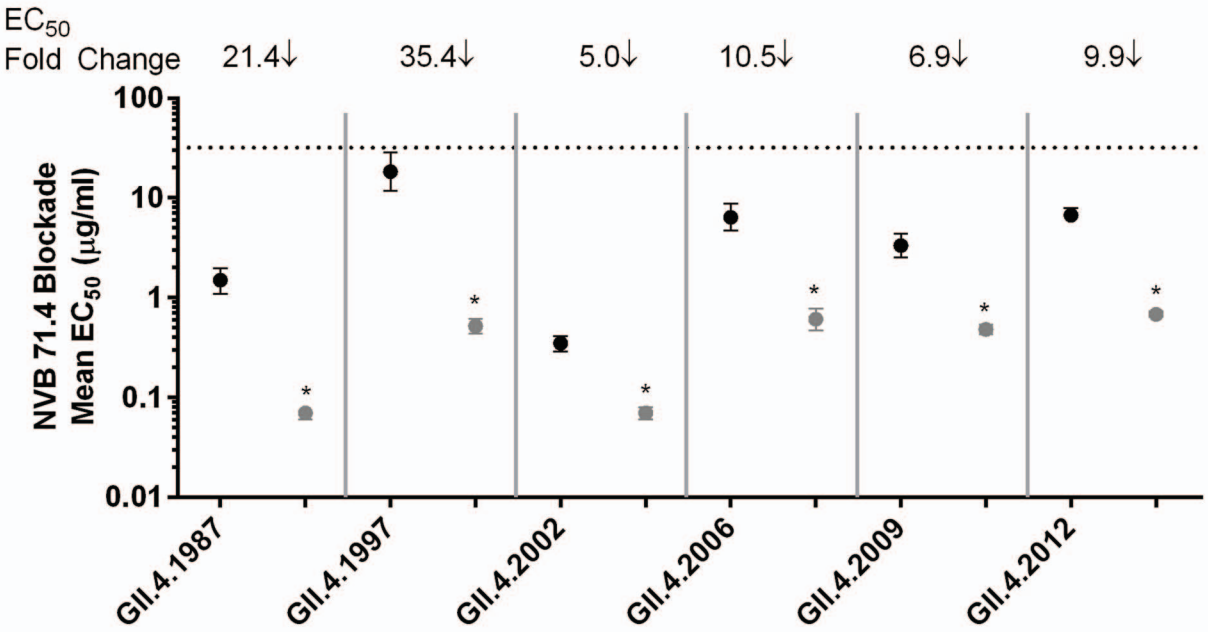

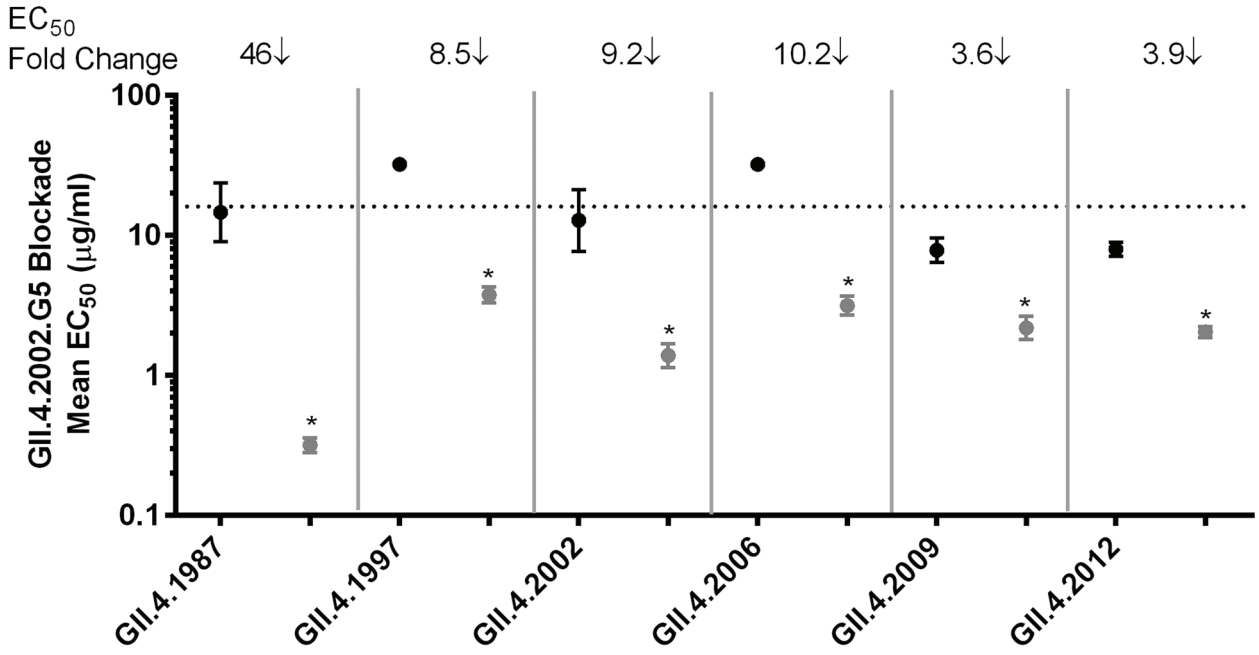

A

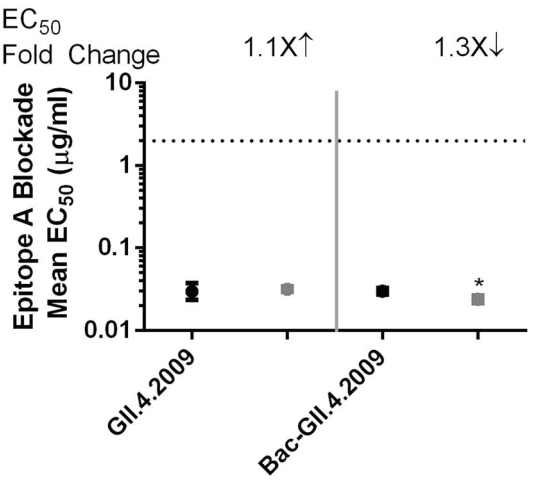

B

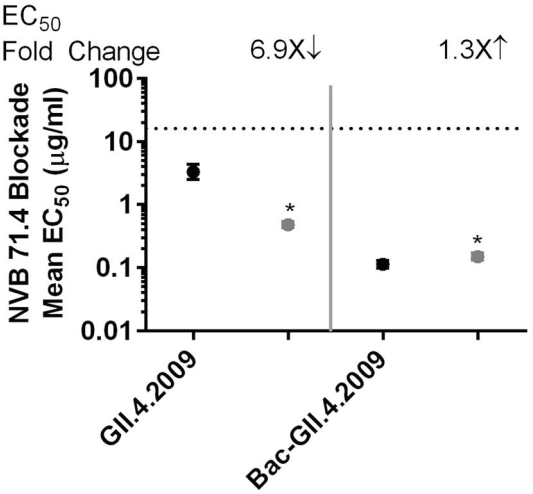

C

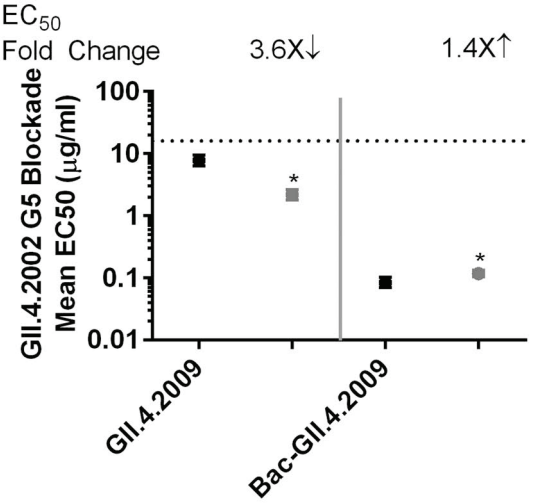

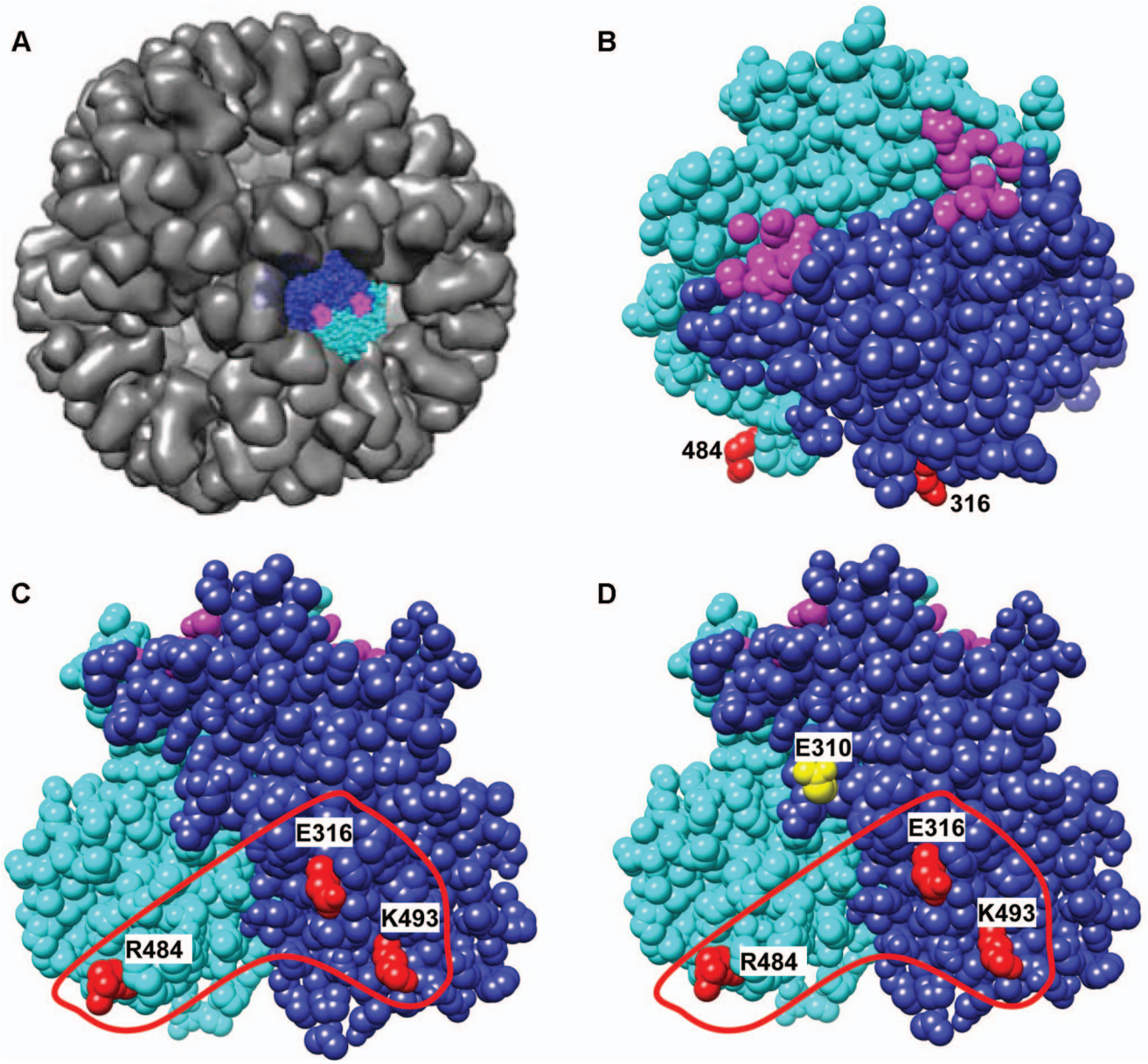

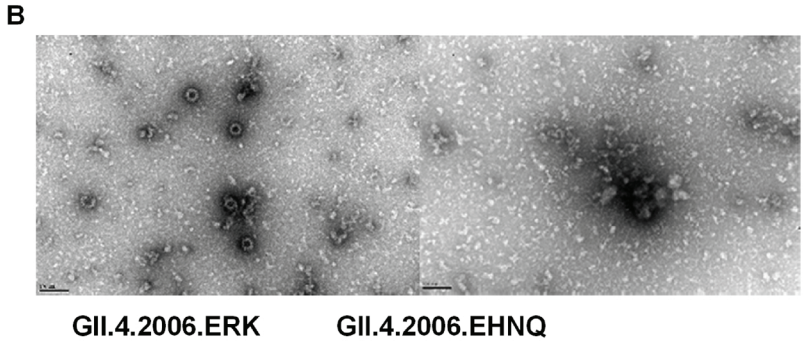

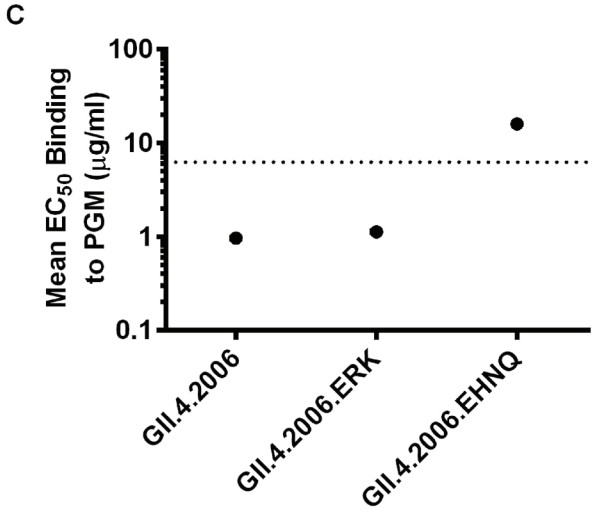

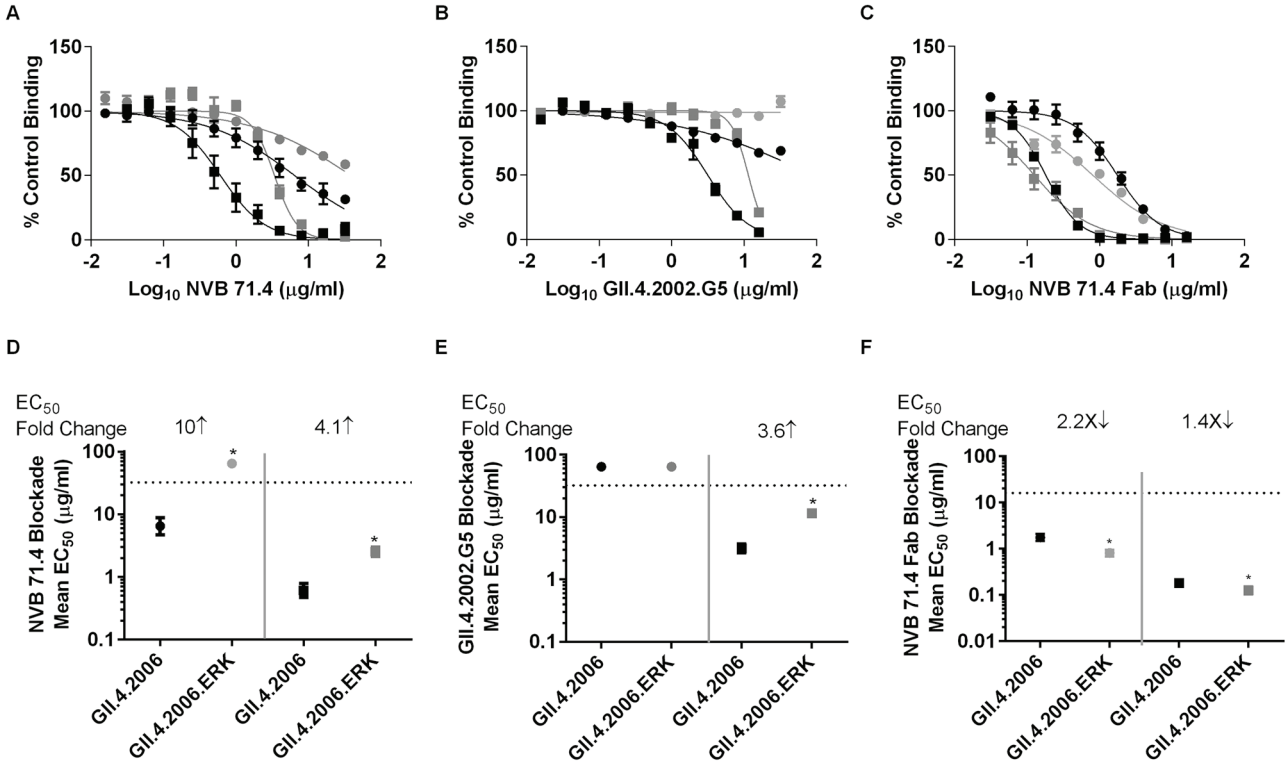

A

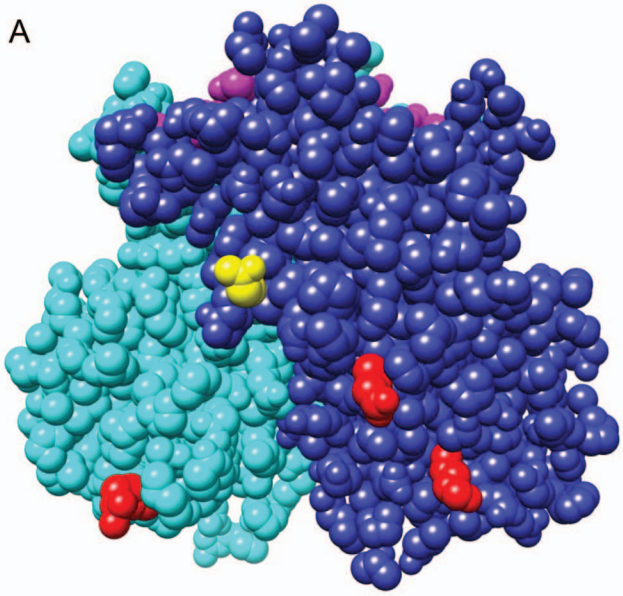

B

	Predicted Motif "NERK"			
VLPs	310	316	484	493
GII.4.1987	N	E	R	K
GII.4.1997	N	E	R	K
GII.4.2002	N	E	R	K
GII.4.2004	N	E	R	K
GII.4.2006	N	E	R	K
GII.4.2009	S	E	R	K
GII.4.2012	D	E	R	K

A

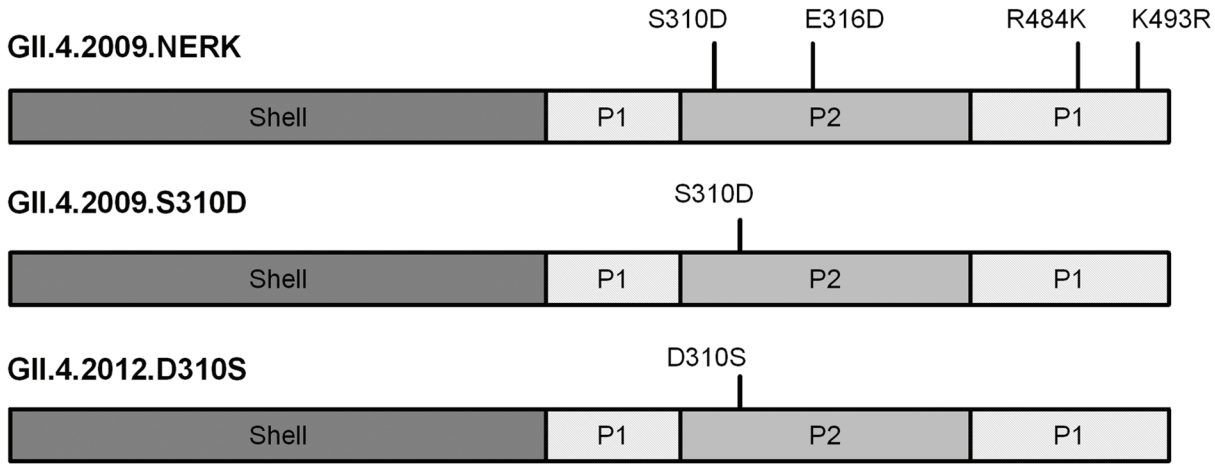

B

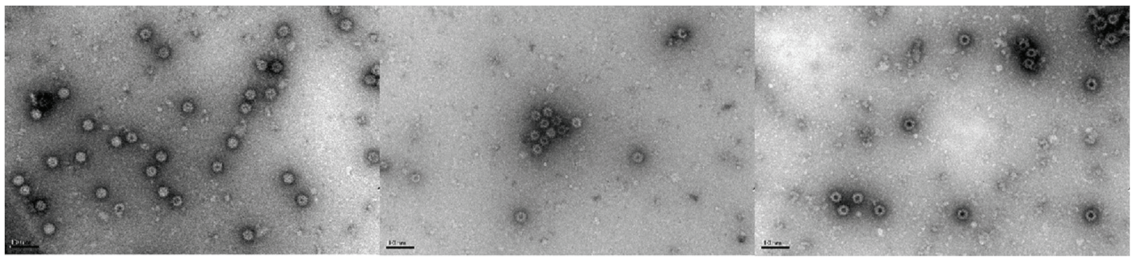

C

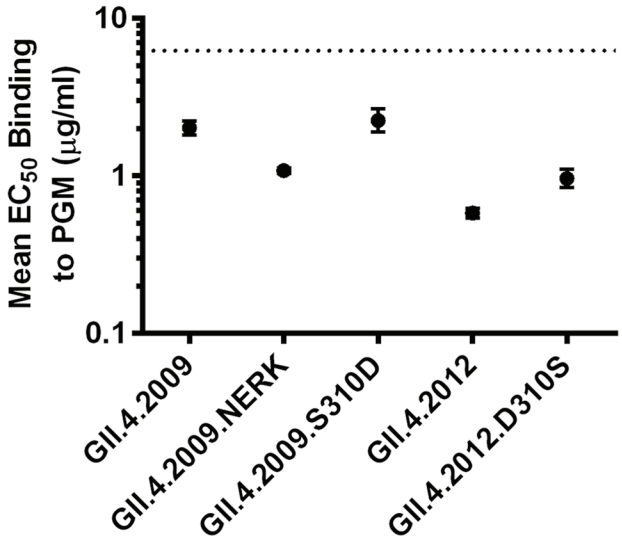

A

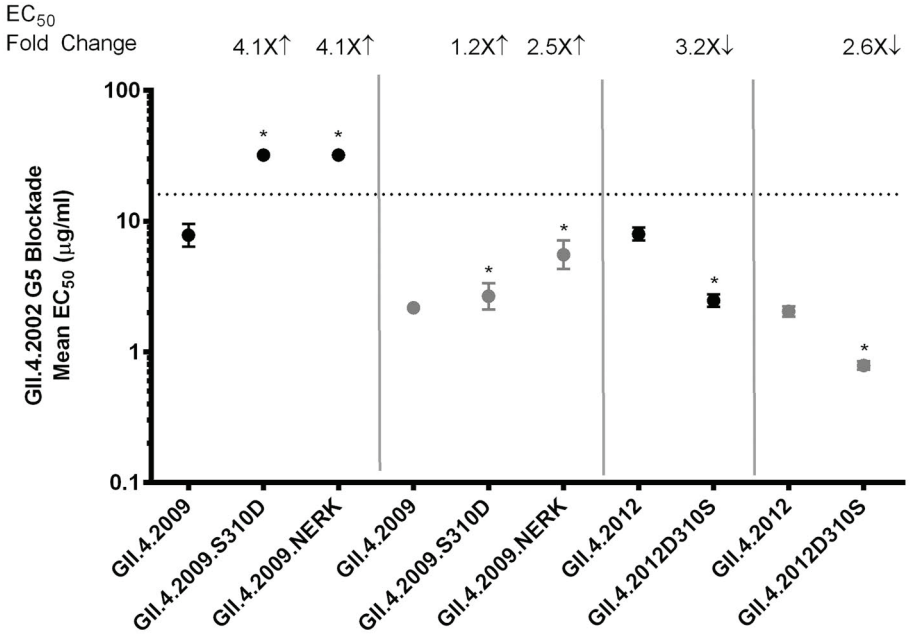

B

mab	NVB 71.4 Fab		NVB 71.4 IgG		GII.4.2002.G5	
VLP	Potency	Temperature Sensitivity	Potency	Temperature Sensitivity	Potency	Temperature Sensitivity
GII.4.2009.S310D	2.8	8.0	2.0	10.5	4.1	12.0
GII.4.2012.D310S	1.0	5.4	2.7	4.6	3.2	3.1
GII.4.2009.NERK	1.0	2.4	1.2	4.6	4.1	5.8